UNIVERSIDAD DE INVESTIGACIÓN DE TECNOLOGÍA EXPERIMENTAL YACHAY

Escuela de Ciencias Biológicas e Ingeniería

TÍTULO: Modeling of UV radiation in Otavalo and Cañaveral (Ecuador), and development of software for the prognosis of skin cancer induced by solar radiation

Trabajo de integración curricular presentado como requisito para la obtención del título de Ingeniería Biomédica

Autores:

Cachiguango Lema Sandra Viviana

Pilco Gualotuña Jhoanna Elizabeth

Tutor:

Ph.D. Salum Graciela

Co-tutor:

Ph.D. Zerpa Levis

Urcuquí, enero 2020

Urcuquí, 13 de mayo de 2020

SECRETARÍA GENERAL
(Vicerrectorado Académico/Cancillería)
ESCUELA DE CIENCIAS BIOLÓGICAS E INGENIERÍA
CARRERA DE BIOMEDICINA
ACTA DE DEFENSA No. UITEY-BIO-2020-00012-AD

A los 13 días del mes de mayo de 2020, a las 11:00 horas, de manera virtual mediante videoconferencia, y ante el Tribunal Calificador, integrado por los docentes:

Presidente Tribunal de Defensa	Dr. ALMEIDA GALARRAGA, DIEGO ALFONSO , Ph.D.
Miembro No Tutor	Dr. BALLAZ GARCIA, SANTIAGO JESUS , Ph.D.
Tutor	Dra. SALUM , GRACIELA MARISA , Ph.D.

El(la) señor(ita) estudiante **CACHIGUANGO LEMA, SANDRA VIVIANA**, con cédula de identidad No. **1003964596**, de la **ESCUELA DE CIENCIAS BIOLÓGICAS E INGENIERÍA**, de la Carrera de **BIOMEDICINA**, aprobada por el Consejo de Educación Superior (CES), mediante Resolución **RPC-SO-43-No.496-2014**, realiza a través de videoconferencia, la sustentación de su trabajo de titulación denominado: **Modeling of UV radiation in Otavalo and Cañaveral (Ecuador), and development of software for the prognosis of skin cancer induced by solar radiation**, previa a la obtención del título de **INGENIERO/A BIOMÉDICO/A**.

El citado trabajo de titulación, fue debidamente aprobado por el(los) docente(s):

Tutor	Dra. SALUM , GRACIELA MARISA , Ph.D.

Y recibió las observaciones de los otros miembros del Tribunal Calificador, las mismas que han sido incorporadas por el(la) estudiante.

Previamente cumplidos los requisitos legales y reglamentarios, el trabajo de titulación fue sustentado por el(la) estudiante y examinado por los miembros del Tribunal Calificador. Escuchada la sustentación del trabajo de titulación a través de videoconferencia, que integró la exposición de el(la) estudiante sobre el contenido de la misma y las preguntas formuladas por los miembros del Tribunal, se califica la sustentación del trabajo de titulación con las siguientes calificaciones:

Tipo	Docente	Calificación
Presidente Tribunal De Defensa	Dr. ALMEIDA GALARRAGA, DIEGO ALFONSO , Ph.D.	10,0
Miembro Tribunal De Defensa	Dr. BALLAZ GARCIA, SANTIAGO JESUS , Ph.D.	10,0
Tutor	Dra. SALUM , GRACIELA MARISA , Ph.D.	10,0

Lo que da un promedio de: **10 (Diez punto Cero)**, sobre 10 (diez), equivalente a: **APROBADO**

Para constancia de lo actuado, firman los miembros del Tribunal Calificador, el/la estudiante y el/la secretario ad-hoc.

Certifico que *en cumplimiento del Decreto Ejecutivo 1017 de 16 de marzo de 2020, la defensa de trabajo de titulación (o examen de grado modalidad teórico práctica) se realizó vía virtual, por lo que las firmas de los miembros del Tribunal de Defensa de Grado, constan en forma digital.*

CACHIGUANGO LEMA, SANDRA VIVIANA
Estudiante

Firmado electrónicamente por: DIEGO ALFONSO ALMEIDA GALARRAGA

Dr. ALMEIDA GALARRAGA, DIEGO ALFONSO , Ph.D.
Presidente Tribunal de Defensa

GRACIELA MARISA SALUM

Firmado digitalmente por GRACIELA MARISA SALUM
Fecha: 2020.07.11 20:44:37 -05'00'

Dra. SALUM . GRACIELA MARISA . Ph.D.
Tutor

SANTIAGO JESUS BALLAZ GARCIA

Firmado digitalmente por SANTIAGO JESUS BALLAZ GARCIA
Fecha: 2020.07.11 11:41:24 -05'00'

Dr. BALLAZ GARCIA, SANTIAGO JESUS , Ph.D.
Miembro No Tutor

Firmado electrónicamente por:
KARLA ESTEFANIA ALARCON FELIX

ALARCON FELIX, KARLA ESTEFANIA
Secretario Ad-hoc

UNIVERSIDAD YACHAY TECH

Urcuquí, 13 de mayo de 2020

SECRETARÍA GENERAL
(Vicerrectorado Académico/Cancillería)
ESCUELA DE CIENCIAS BIOLÓGICAS E INGENIERÍA
CARRERA DE BIOMEDICINA
ACTA DE DEFENSA No. UITEY-BIO-2020-00013-AD

A los 13 días del mes de mayo de 2020, a las 11:00 horas, de manera virtual mediante videoconferencia, y ante el Tribunal Calificador, integrado por los docentes:

Presidente Tribunal de Defensa	Dr. ALMEIDA GALARRAGA, DIEGO ALFONSO , Ph.D.
Miembro No Tutor	Dr. BALLAZ GARCIA, SANTIAGO JESUS , Ph.D.
Tutor	Dra. SALUM , GRACIELA MARISA , Ph.D.

El(la) señor(ita) estudiante **PILCO GUALOTUÑA, JHOANNA ELIZABETH**, con cédula de identidad No. **1726530734**, de la **ESCUELA DE CIENCIAS BIOLÓGICAS E INGENIERÍA**, de la Carrera de **BIOMEDICINA**, aprobada por el Consejo de Educación Superior (CES), mediante Resolución **RPC-SO-43-No.496-2014**, realiza a través de videoconferencia, la sustentación de su trabajo de titulación denominado: **Modeling of UV radiation in Otavalo and Cañaveral (Ecuador), and development of software for the prognosis of skin cancer induced by solar radiation**, previa a la obtención del título de **INGENIERO/A BIOMÉDICO/A**.

El citado trabajo de titulación, fue debidamente aprobado por el(los) docente(s):

Tutor	Dra. SALUM , GRACIELA MARISA , Ph.D.

Y recibió las observaciones de los otros miembros del Tribunal Calificador, las mismas que han sido incorporadas por el(la) estudiante.

Previamente cumplidos los requisitos legales y reglamentarios, el trabajo de titulación fue sustentado por el(la) estudiante y examinado por los miembros del Tribunal Calificador. Escuchada la sustentación del trabajo de titulación a través de videoconferencia, que integró la exposición de el(la) estudiante sobre el contenido de la misma y las preguntas formuladas por los miembros del Tribunal, se califica la sustentación del trabajo de titulación con las siguientes calificaciones:

Tipo	Docente	Calificación
Presidente Tribunal De Defensa	Dr. ALMEIDA GALARRAGA, DIEGO ALFONSO , Ph.D.	10,0
Miembro Tribunal De Defensa	Dr. BALLAZ GARCIA, SANTIAGO JESUS , Ph.D.	10,0
Tutor	Dra. SALUM , GRACIELA MARISA , Ph.D.	10,0

Lo que da un promedio de: **10 (Diez punto Cero)**, sobre 10 (diez), equivalente a: **APROBADO**

Para constancia de lo actuado, firman los miembros del Tribunal Calificador, el/la estudiante y el/la secretario ad-hoc.

Certifico que *en cumplimiento del Decreto Ejecutivo 1017 de 16 de marzo de 2020, la defensa de trabajo de titulación (o examen de grado modalidad teórico práctica) se realizó vía virtual, por lo que las firmas de los miembros del Tribunal de Defensa de Grado, constan en forma digital.*

PILCO GUALOTUÑA, JHOANNA ELIZABETH
Estudiante

DIEGO ALFONSO ALMEIDA GALARRAGA

Dr. ALMEIDA GALARRAGA, DIEGO ALFONSO , Ph.D.
Presidente Tribunal de Defensa

UNIVERSIDAD YACHAY TECH

GRACIELA MARISA SALUM

Firmado digitalmente por GRACIELA MARISA SALUM
Fecha: 2020.07.11 20:44:14 -05'00'

Dra. SALUM , GRACIELA MARISA , Ph.D.
Tutor

SANTIAGO JESUS BALLAZ GARCIA

Dr. BALLAZ GARCIA, SANTIAGO JESUS , Ph.D.
Miembro No Tutor

KARLA ESTEFANIA ALARCON FELIX

ALARCON FELIX, KARLA ESTEFANIA
Secretario Ad-hoc

AUTORÍA

Yo, **Sandra Viviana Cachiguango Lema**, con cédula de identidad 1003964598,declaro que las ideas, juicios, valoraciones, interpretaciones, consultas bibliográficas, definiciones y conceptualizaciones expuestas en el presente trabajo: así cómo, los procedimientos y herramientas utilizadas en la investigación, son de absoluta responsabilidad de la autora del trabajo de integración curricular. Asi mismo, me acojo a los reglamentos internos de la Universidad de Investigación de Tecnología Experimental Yachay.

Urcuquí, Julio 2020

Sandra Viviana Cachiguango Lema
1003964598

AUTORÍA

Yo, **JHOANNA ELIZABETH PILCO GUALOTUÑA**, con cédula de identidad 1726530734, declaro que las ideas, juicios, valoraciones, interpretaciones, consultas bibliográficas, definiciones y conceptualizaciones expuestas en el presente trabajo; así cómo, los procedimientos y herramientas utilizadas en la investigación, son de absoluta responsabilidad de el/la autora (a) del trabajo de integración curricular. Así mismo, me acojo a los reglamentos internos de la Universidad de Investigación de Tecnología Experimental Yachay.

Urcuquí, julio, 2020.

Jhoanna Pilco

Jhoanna Elizabeth Pilco Gualotuña
CI: 1726530734

AUTORIZACIÓN DE PUBLICACIÓN

Yo, **Sandra Viviana Cachiguango Lema**, con cédula de identidad 1003964598, cedo a la Universidad de Investigación de Tecnología Experimental Yachay, los derechos de publicación de la presente obra, sin que deba haber un reconocimiento económico por este concepto. Declaro además que el texto del presente trabajo de titulación no podrá ser cedido a ninguna empresa editorial para su publicación u otros fines, sin contar previamente con la autorización escrita de la Universidad.

Asimismo, autorizo a la Universidad que realice la digitalización y publicación de este trabajo de integración curricular en el repositorio virtual, de conformidad a lo dispuesto en el Art. 144 de la Ley Orgánica de Educación Superior

Urcuquí, Julio 2020

Sandra Viviana Cachiguango Lema
1003964598

x

AUTORIZACIÓN DE PUBLICACIÓN

Yo, **JHOANNA ELIZABETH PILCO GUALOTUÑA,** con cédula de identidad 1726530734, cedo a la Universidad de Investigación de Tecnología Experimental Yachay, los derechos de publicación de la presente obra, sin que deba haber un reconocimiento económico por este concepto. Declaro además que el texto del presente trabajo de titulación no podrá ser cedido a ninguna empresa editorial para su publicación u otros fines, sin contar previamente con la autorización escrita de la Universidad.

Asimismo, autorizo a la Universidad que realice la digitalización y publicación de este trabajo de integración curricular en el repositorio virtual, de conformidad a lo dispuesto en el Art. 144 de la Ley Orgánica de Educación Superior

Urcuquí, julio, 2020.

Jhoanna Pilco

Jhoanna Elizabeth Pilco Gualotuña
CI: 1726530734

Dedication

This project is dedicated to my parents María Olga and José, and my brother Elvis, who were my mainstay in the most difficult moments during my university career. Also, I thank my friends for their support, love and I will always carry them in my heart.

Sandra Cachiguango

This project is dedicated to my mother, my guardian angel, for the teachings she left me, which have helped me overcome all kinds of obstacles. To Rosario, Blanca, Carmen, Segundo, and Víctor, for their affection, care, support, and love. I can say that they have become my second mothers and fathers. Finally, to my friends for all the moments shared. Thanks to them, Yachay was one of the best stages of my life. I will always remember them and carry them around my heart.

Jhoanna ELizabeth Pilco Gualotuña

Acknowledgment

We would like to express our deep gratitude to our advisor, Graciela Salum, for her patience guidance and advice throughout the development of this project. We would also like to thank Dr. Cecilia Cañarte for dermatological care center Cadermint SA for her advice and assistance in solving our doubts. Finally, we wish to thank our teachers, family and friends for their support, and encouragement throughout our studies.

Sandra Cachiguango y Jhoanna Pilco

Resumen

Ecuador, debido a su posición geográfica, recibe radiación solar directamente, por lo que el cáncer de piel tipo melanoma y no melanoma adquieren una relevancia especial. El cáncer de piel puede invadir otros órganos vitales, por lo que la detección temprana es esencial ya que aumenta las posibilidades de curación de los pacientes. No hay datos registrados sobre la intensidad de la radiación o la incidencia de lesiones dérmicas. El método automático es un método visual computacional utilizado para detectar cáncer de piel. En esta tesis, se propuso, en primer lugar, analizar la relación de la radiación solar y el cáncer de piel modelando la radiación solar de dos ciudades en Ecuador (Otavalo y Cañaveral), y el espectro de acción del daño del ADN. Los datos de los siete parámetros utilizados para determinar la radiación solar obtenidos de tres bases de datos fueron Giovanni/NASA, NASA Power y NOAA Earth System Research. Los resultados muestran que, de hecho, Otavalo presenta un mayor riesgo de desarrollar cáncer de piel debido a la alta irradiancia solar que muestra esta ciudad. Luego, procedimos a encuestar a personas de Otavalo para determinar su nivel de conocimiento sobre cáncer de piel. Esta encuesta se realizó a 50 personas de Otavalo que trabajan en la Plaza de los Ponchos, obteniendo que el 88% conoce sobre cáncer de piel y la radiación solar como un factor en el desarrollo de esta enfermedad. Sin embargo, la mayoría de ellos no aplican medidas adecuadas de protección solar. Finalmente, se ha propuesto un software para el pronóstico del cáncer de piel basado en el procesamiento de imágenes de lesiones cutáneas (manchas, lunares) y el uso de una red neuronal convolucional para la extracción de características y su clasificación en las cuatro clases seleccionadas: carcinoma de células basales, tumores benignos, melanoma y carcinoma de células escamosas. Los resultados obtenidos fueron una precisión de 0,66, una sensibilidad de 0,31 y una especificidad de 0,77. Finalmente, se espera mejorar los resultados en futuros trabajos para crear una aplicación móvil accesible para el usuario que indique el posible riesgo de cáncer de piel y ayude a su acercamiento con el dermatólogo para comenzar el tratamiento adecuado.

Palabras claves: Cáncer de piel, melanoma, no melanoma, dermatología, radiación solar.

Abstract

Ecuador, due to its geographical position, receives solar radiation directly, so melanoma and non-melanoma skin cancer have a particular connotation. Skin cancer can invade other vital organs, so early detection is essential because it increases the chances of cure in patients. There are no recorded data on the intensity of the radiation or the incidence of dermal lesions. The automatic method is a computational visual method used to detect skin cancer. In this thesis, it proposed, first, to analyze the relationship of solar radiation and skin cancer by modeling solar radiation from two cities in Ecuador (Otavalo and Cañaveral), and the DNA damage action spectrum. The data of the seven parameters used to determine solar irradiance obtained from three databases were Giovanni NASA, NASA POWER, and NOAA Earth System Research. The results show that, indeed, Otavalo presents a higher risk of developing skin cancer due to the high solar irradiance that this city shows. Then, we proceed to survey Otavalo people to determine the level of knowledge about skin cancer. This survey carried out on the 50 Otavalian people who working outdoor in the Plaza de Los Ponchos. It turned out that 88% of survey participants knew about solar radiation as a risk factor for skin cancer. However, most of them did not take adequate measures for sun protection. Herein, a software for the prognosis of skin cancer has proposed-based in the processing of images of skin lesions (spots, moles), and the use of a convolutional neural network for the extraction of characteristics and their classification in the four selected classes - basal cell carcinoma, benign tumors, melanoma and squamous cell carcinoma. The results obtained were accuracy of 0.66, a sensitivity of 0.31, and a specificity of 0.77. Finally, it has expected to improve the results in future works to create a mobile application accessible to the user that indicates the possible risk of skin cancer and help your approach with the dermatologist to begin the appropriate treatment.

Keywords: Skin cancer, melanoma, non-melanoma, dermatology, solar radiation.

Table of Contents

Tables List

List of figures

1 Introduction

1.1 Problematic statement

Skin cancer cases have incremented over the last years (1)(2). It takes place when skin cells divide uncontrollably. There are two types: melanoma, and non-melanoma (squamous cell carcinoma, or basal cell carcinoma). The first occupies the nineteenth and the second occupies the fifth place of the most common cancers around the world (3). One of the factors involved in the development of skin cancer is exposure to terrestrial ultraviolet (UV) radiation that covers a range from 290 to 400 nm wavelength bands (4),(5). UV radiation carries energy in the form of photons, and these are absorbed by chromophores compounds (nucleic acids and proteins), producing biochemical reactions that alter the cell (photo damage)(6). UVB causes DNA lesions and induces skin cancer due to its high energy level (7). People with a low levels of melanin in the epidermis tend to frequently develop skin cancer, although at rates that change depending on age, location, ethnicity, and photoaging (8) (9). UV radiation is affected by factors such as ozone content, altitude, aerosols, albedo, among others (10). Stratospheric ozone is a beneficial absorber of UV radiation that acts as a filter and determines the amount of radiation that reaches Earth's surface (7).

Non-melanoma cancers (basal and squamous cell carcinomas) are the most common types of skin cancer, and melanoma makes up only 1% of skin cancer cases, although with a high mortality rate because of metastasis (2). According to the American Cancer Society (11), about 5.4 million Americans are diagnosed with non-melanoma skin cancer; and 100350 cases with melanoma, 6850 of which are expected to be life-threatening (2). Although there are no current statistics on how many cases of skin, melanoma and non-melanoma, occur annually in Ecuador, it is believed that the incidence rate of melanoma (Known by incident rate as the number of skin cancer cases divided by the population at risk in one place and during a specific period (12)) is increasingly higher. The latest official National Tumor Registry of Guayaquil (13) reports 19,680 cases of cancer from 2014 to 2018, which of 9.3% correspond to skin cancer in men and 6% to skin cancer in women. Accordingly, skin cancer is likely to be one of the five types of cancers with the highest incidence in Ecuador. The reason may be the localization of Ecuador in the equinoctial line, which predisposes its population to the development of this cancer (14). Despite this, there is lack of public health policies and prophylactic measures to prevent population from developing this cancer in Ecuador. For instance, quantitative data on the net dose of UV radiation that averaged population receives is scarce. People is also unaware of the risks of being exposed to sun radiation for hours. It is common to observe people outdoors without any sun protection due to ignorance about skin cancer or perhaps because of the costs of sun block creams and sunglasses. Another factor is the frequency at which Ecuadorians are seen by a dermatologist.

Based on all the above, this thesis had two objectives. Firstly, to generate data and information about the amount of solar UV radiation by sun for education purposes. For this reason, UV radiation modelling was carried out in Otavalo and Cañaveral using the SMART295 software. In addition, surveys were also conducted to determine the level of knowledge of the risk of skin cancer and how to prevent it among population. Second, to design a skin cancer detection software able to automatically classify skin lesions between benign lesions and severe skin cancers (either squamous, basal or melanoma), based on a convolutional neural network that uses a set of skin cancer images as a reference to compare them with suspicious skin spots, and thus to quickly inform the user of the risk for developing skin cancer. The goal is to promptly alert the user of the putative risk of having that sun-induced skin lesions.

1.2 Objectives

1.2.1 General Objective

To decrease the incidence of skin cancer through (1) the development of an application for the prognosis of skin cancer and (2) the study of the levels of solar radiation as a function of the DNA damage as an approach to the risk for having skin cancer in Ecuador.

1.2.2 Specific Objectives

- A survey among the dwellers of Otavalo regarding their awareness of skin cancer and its prevention.
- The analysis of the relationship between spectral ultraviolet solar radiation measured in Otavalo and Cañaveral and the DNA damage action spectrum as an estimation of the risk for developing skin cancer in Ecuador.
- The design of an automatic software to promptly detect and prevent skin cancer based on image processing and a simple convolutional neural network in Python a programming language.

1.3 Background

The Skin Cancer Foundation (1) defines skin cancer as an uncontrollable growth of cells that can become cancer cells. It can be cured at very high rates with simple and economical treatments if detection is early (15). Skin cancer can be classified into two types. Melanoma originates in a type of cell called melanocyte and non-melanoma that can originate at basal or squamous cells, as shown in figure 1.

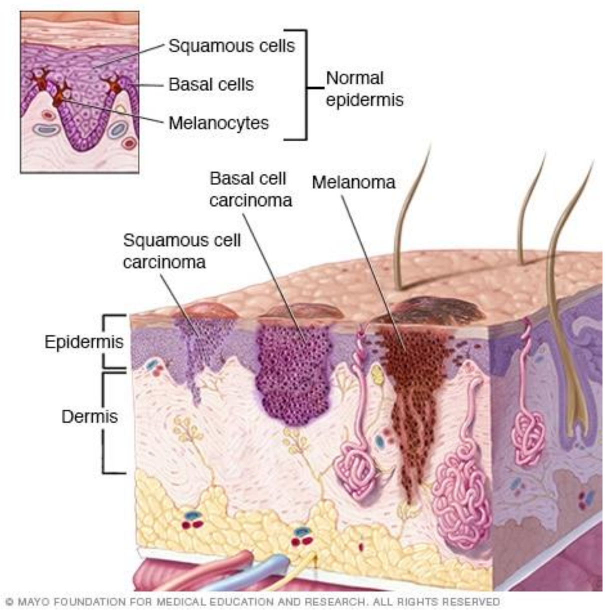

Figure 1. Cells involved in skin cancer and schematic of types of skin cancer (16)

1.3.1 Non-melanoma Skin Cancer

Within skin cancer types, non-melanoma is the most frequency and is related to exposure to UV rays (17). This type of cancer is more common in skin phototype, ability of the skin to assimilate solar radiation, mostly equal or lower than III (7). Also, factors as ethnicity, photoaging, age, or geographic location (lower altitude, greater exposure to UV radiation) can change the rate related to skin phototype (8), (18). In Ecuador, nonmelanoma skin cancer prevalence is higher in people over 50 years. Also, this type of cancer can reappear in the same area that was first found, and it can be seen as spots or ulcers that cause itching and can bleed easily (19). Non-melanoma skin cancer encompasses two types of tumors: squamous, and basal cell carcinoma. Also, other types of non-melanoma like Merkel cell carcinoma, cutaneous lymphoma, hair follicle tumors, and Kaposi sarcoma affect 1% of the skin cancers total (4).

1.3.1.1 Squamous cell carcinoma (SCC)

SCC is characterized by the presence of a flat lesion with a scaly surface and a red nodule (Fig 2). SCC is a common malignant tumor originating from epidermal keratinocytes, and it is the second most frequent after basal cell carcinoma (15) (8). Although the SCC incidence is difficult to estimate because there is not statistic record (20) (21), it increases after the age of 40, being two to three times more common in old men. The development of SCC is produced by multiple factors such as human papillomavirus and immunodeficiency virus infections, chronic skin inflammation, burn scars, smoking, and chronic arsenic exposure, and overall by the cumulative exposure to UV rays (21) (8).

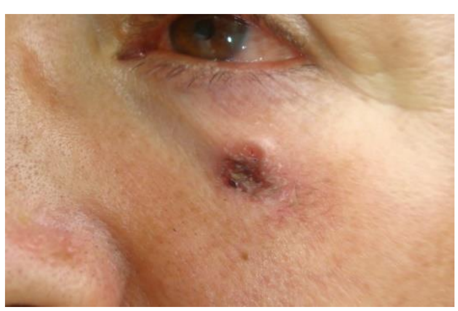

Figure 2.An ilustrative case of Squamoso Cell Carcinoma or SCC. Source: Dr. Cecilia Cañarte.

1.3.1.2 Basal cell carcinoma (BCC).

It has a flat scar-like lesion, waxy or profiled lump, and an ulcer with blood that heals and returns and that are evidenced mainly in areas exposed to the sun (Fig.3) Keranocytes in the basal cell layer are the origin of BCC and generally does not metastasize, so it is rarely fatal. Nevertheless, BCC might also be locally aggressive and invade nearby structures (22) (21). According to the American Cancer Society (4), 8 out of 10 cases of skin cancer are BCC.

Figure 3. A case of Basal Cell Carcinoma (BCC) in the nose. Source: Dr. Cecilia Cañarte.

The main risk factor for BCC development is the exposure to UV light. The risk for BCC is directly related to the level of skin pigmentation, being more common in white (Caucasian race) people than in people with dark pigmented (Mixel race) skin (1).

1.3.2 Melanoma skin cancer

Melanoma has a large area with irregular borders and parts that appear red, pink, white, dark blue pigmentation. It is the most dangerous form of skin cancer and it develops in melanocytes (15). Unlike nonmelanoma skin cancer, melanoma has a great ability to metastases, which makes it one the most aggressive cancers (23). Early detection is critical to achieve a high percentage of cure of this cancer.

Most melanoma (Fig. 4) have brown or black spots due to the presence of melanin, but there are cases of melanomas that look pink or even white and this is because melanoma does not produce enough melanin (24). Most cases of melanoma are painless. However, melanoma also produce dark and painful lesion in palms, soles, fingertips; and even in mucous surfaces of the mouth, nose, vagina and anus (25).

Figure 4. Nodular melanoma on the edge of the foot. Source: Dr. Cecilia Cañarte.

Most cases of melanoma cancer are of *de novo* origin, and only 20% are caused by previous nevus lesions (26). Excessive exposure to UV light seems to contribute to the incidence and mortality of melanoma. Other risk factors include white skin, history of sunburn, living near the equator, age, immunosuppression, family history of melanoma, multiple nevi (15).

The characteristics of the above-mentioned skin cancers are summarized in table I.

Table 1. Characteristics of the different types of skin cancer. Source: Prepared by authors.

Types of skin cancer	Definition	Frequency	Mortality	Cause
Squamous cell carcinoma (SCC)	Common malignant tumors originating from epidermal keratinocytes	Second most frequent	Medium	-UV radiation (80%) -Infections: HPV, HIV -Burn scars, smoking -Chronic skin exposure
Basal Cell Carcinoma (BCC)	Cancer that originates from keratinocytes in the basal layer of the epidermis	First most frequent	Low	-UV radiation (80%) -Burn scars -Ionizing radiation -Chronic skin exposure
Melanoma	It develops in melanocytes (cells that produce melanin pigment)	Less frequent	High	-UV radiation -History of sunburn -Living near the equator (higher altitude, lower latitude) -Multiple nevi

1.3.3 Dermatological procedures for the diagnosis of skin cancer

Skin cancers detect by examining characteristics of the lesion such as size, colour, texture. However, each type of skin cancer has different features. For example, BCC has areas with flushed or pink bumps that are continually growing or are healing and reappearing. This type of cancer is fragile and may bleed from what is seen like open sores. SCC also has reddened bumps but has a rough or scaly texture similar to warts. Concerning melanoma, it does not bleed early stage so that dermatologists have to apply the “ABCD” rule for appropriate diagnosis (27). This acronym refers to four criteria: asymmetry, border irregularity, color, and diameter (28), which are listed below.

- *Asymmetry*. It is when half of the abnormal area is different from the other half and is generated by the uncontrolled growth of the lesion (25).
- *Edge*. The borders are analyzed according to the sharpness of the edge. Melanocytic lesions have pronounced or sharp edges at their ends (29).

- *Color.* The color is related to the excess melanin under the surface of the lesion. There are six different colors, which are black, red, light brown, dark brown, blue-gray, black (25).
- *Diameter***.** The mole has a diameter greater than 0.63 cm (28).

Another parameter no mentioned above is evolution, which relates to the change of the mole in the shape and its elevation over the skin (30).

Some other method used for the diagnosis of melanoma skin cancer is AJCC, which describes the extent of disease progression. The American Joint Committee on Cancer developed this system, and it is based on TNM: Tumor size, Lymph Nodes affected, Metastases (31).

1.3.4 Computer- based tools for skin cancer prognosis

Early diagnosis of the melanoma cancer depends on how much a clinical eye is prepared to early distinguish it, which the increases the probability of survival by 95% (29). The identification of skin cancer quickly and effectively is a challenge even for an experienced dermatologist. Automated analysis of pigmented skin lesions has become a research field that has gained a growing interest, which has led to the development of tools for computer-assisted diagnosis of skin cancers. Computer vision or artificial vision for melanoma detection "includes methods to obtain, process, analyze and understand real-world images to produce numerical or symbolic information so that a computer can treat them" (32). Computer-based tools are being developed to aid professionals deal with skin cancers (33). Cavalcanti et al. (28) proposed a system consisting of an image pre-processing, segmentation, feature extraction based on the ABCD criteria and a classification based on k-Nearest Neighbours (KNN) showing a sensitivity of 89.72% and specificity of 75.56%. Another study published in Symmetry by Kalwa and colleagues (34) developed software focused on the extraction of ABCD characteristics through image capture, preprocessing, and segmentation. The malignancy of the tumor was detected using the support vector machine classifiers (developed in-house) with a sensitivity of 80%, specificity of 90%, and an accuracy of 88% obtained on 200 dermatoscopic images tested.

As shown in Figure 5, image acquisition, pre-processing, segmentation, feature extraction, and classification are key components in the classification via computer vision-based diagnosis of melanoma.

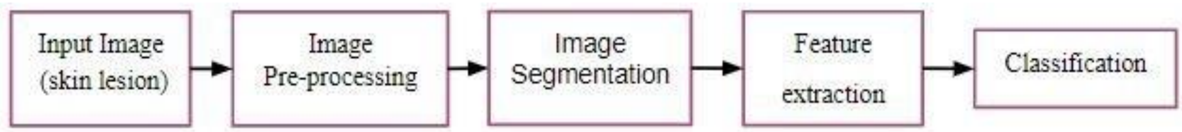

Figure 5. Flux diagram of the computer-assisted melanoma detection system. Source: Prepared by authors.

The diagnostic system, as stated above, is actually a consuming-time and challenging task, so the process requires to be optimized. In this vein, deep learning techniques are being tested for the automatic extraction of features of skin cancers with detection purposes. Based on previously learned skin cancer imaging, deep neural networks take data sets as the input to automatically perform preprocessing, segmentation, and design of handcrafted features of the sample inside the neural network. Consequently, it reduces working time, chances of error, to increase the acuity of prognosis (35), (36). For example, a study uses Inception v3, which is a deep convolutional neural network to classify skin images between benign and melanoma. Esteva and his colleagues (37) used 129,450 clinical images to train the network. Then, CNN showed a high performance in the classification when comparing the results obtained with the analysis of 21 certified dermatologists in clinical images taken by biopsy (38), (39). In another study, two problems related to the use of neural network to classify images of skin lesions are solved by Nasr-Esfahani et al. (40). First, convolutional neural networks (CNN) can be misled by noise caused by illumination artifacts or other noise effects, which were corrected with a preprocessing step. Second, a technique called data augmentation solves the problem of scarcity of skin lesion images with the help of three transformations - scaling, rotation, and cropping. Because of that, 170 images increased to 6120 images. As a result, the team obtained an accuracy of 81% in the classification of melanoma and melanocytic nevus.

1.4 Study Structure

Following the established objectives, the rest of the document has been structured in the subsequent sections.

First, Chapter 2 is dedicated to present the method and results of the survey conducted in the city of Otavalo to the people who work in the Plaza de Los Ponchos. This chapter aims to investigate whether the Otavalo population applies sun protection measures, how much knowledge do they have about solar radiation. Likewise, in the survey is proposed an application (software) for a timely diagnosis of skin abnormalities, and with this, we investigated whether the population would be interested in using an application for this purpose.

Chapter 3 presents the data of the UV radiation modeling in Otavalo and Cañaveral. It is beginning with basic concepts about radiation, factors that affect radiation, solar spectral UV irradiance, and Action Spectrum of DNA damage. These concepts are intended to briefly expose the more general aspects of solar radiation and then focus on the analysis of solar irradiance and solar irradiance to damage DNA. Later, the methodology used and the results obtained are explained.

Chapter 4 focuses on the software proposed in this thesis for the previous diagnosis of skin cancer. This chapter includes a brief description of basic concepts like artificial intelligence, biological neural networks vs. artificial neural networks, and the parts of a neural network. Then, the methodology and results obtained for the two parts of the proposed method, image preprocessing and the convolutional neural network (CNN) model, are presented. Besides, the graphical user interface for the software is also presented in this chapter.

Finally, Chapter 5 concludes the document and mentions future work.

2 Survey

Although Ecuador has high solar radiation that favors the development of skin cancer, many people underestimate the danger of sunburns. In the Andean region, people have usually been seen without hats, long-sleeved clothes, and without sunscreen walking at noon; despite being the region with the highest incidence of radiation. To clarify this lack knowledge about the dangers of unprotected sun exposure was necessary to conduct a survey related to skin cancer and skincare to Otavalo people, specifically people who work in the "Plaza de Los Ponchos" market. Plaza de Ponchos, a place where handicrafts are sold and the main tourist site of Otavalo. The survey is carried out in this place because local people spend outdoors most of the daylight time.

2.1 Methodology

This study is transactional-exploratory since the survey was carried out in a single moment and was explored to a local community. The design of the survey was personal, so there was an interaction between pollster and respondent. Besides, the study was of an analytical type since it sought to investigate and analyze whether the population knows about skin cancer, solar radiation as the main factor to develop this type of cancer, and education in sun protection.

Surveys were conducted about skin cancer and sun protection to people from the Otavalo city, specifically on the people who work in the Plaza de los Ponchos which are people who is exposes to solar radiation longer, in order to estimate the knowledge in these topics. Fifty people aged 12 to 63 years answered the survey. The survey consisted of 15 multiple-choice questions found in Annex 1. Also, informational leaflets about sun protection and skin cancer prevention provided by Dr. Cecilia Cañarte of the Center for Dermatological Integral Cadermint SA were delivered, which found in Annex 2.

2.2 Results and discussion

The results presented in Figure 6 show the number of people surveyed divided by gender and age. The surveys are 31 women, 19 men aged between 12 and 60 years. 64% of respondents live in an urban area, the city of Otavalo, and very few have completed their higher education. Besides, 60% are purely artisans, 28% are artisans - students, 6% are housewives - artisans, 2% public employees, 2% of teachers and 2% journalists (Fig. 7). It is worth mentioning that these last three sell crafts in the Plaza de Los Ponchos, but only on Saturday, the day of the big craft fair.

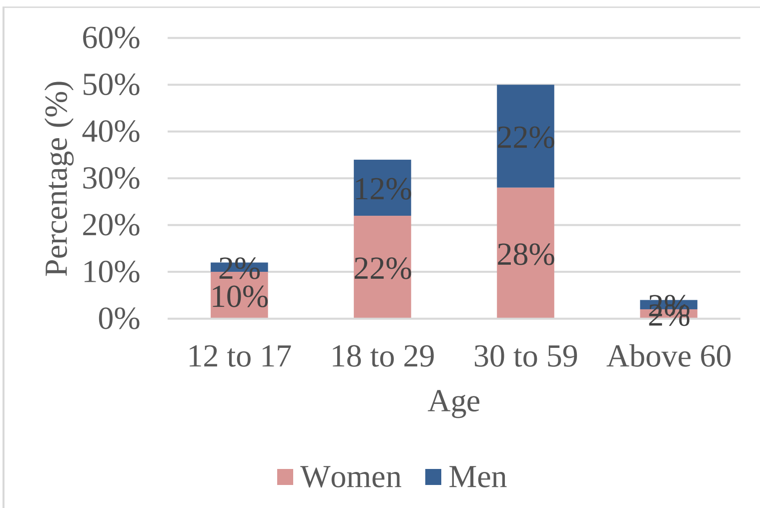

Figure 6. Numbers and percentages of respondents divided by gender and age. Source: Prepared by authors.

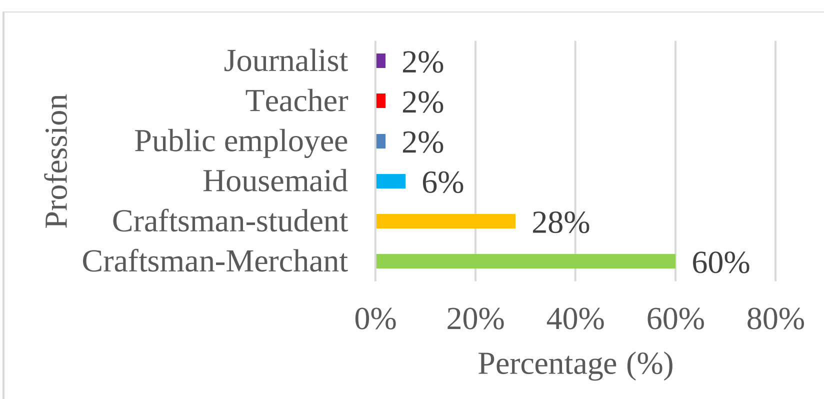

Figure 7. Occupation survey. Source: Prepared by authors.

On the other hand, Figure 8 clearly shows that 88% of surveyed know about skin cancer; a high percentage of them have the right level of knowledge about this topic. However, only 68% of respondents know that the accumulation of solar radiation is the main factor for the development of skin cancer in adults; the data can see in Figure 9. Likewise, surveyed people were asked how often they got sunburns. The survey showed that 46% of respondents used to get sunburn very quickly, 44% sometimes, and only 10% rarely had a sunburn (Fig. 10).

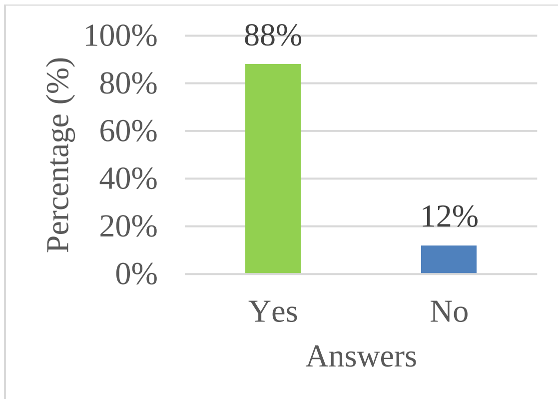

Figure 8. Grade of knowledge of skin cancer. Source: Prepared by authors.

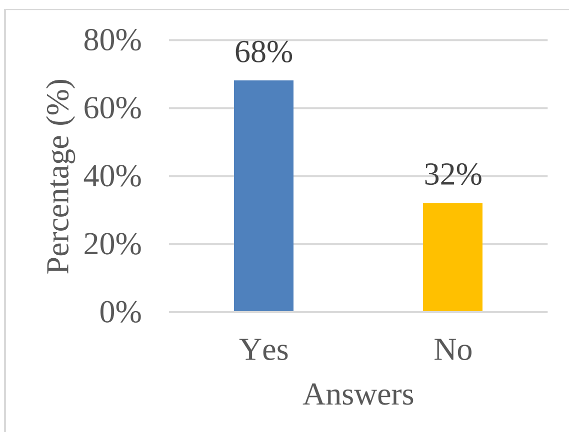

Figure 9. Knowledge about the development of skin cancer by the cumulative sunbathe effects. Source: Prepared by authors.

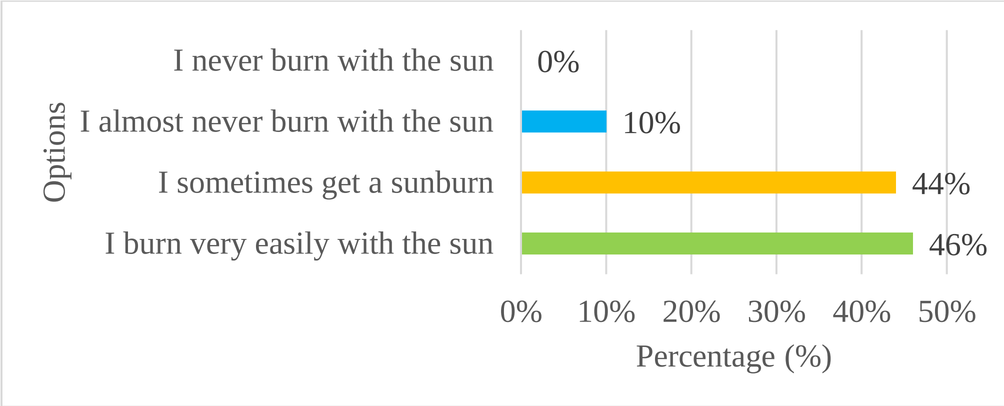

Figure 10. How often people got skin sunburns. Source: Prepared by authors.

90% of respondents protected themselves from the sun (Fig. 11). Also, as seen in Fig 12, the most commonly used protective measures are the use of the hat (76%), walking under the shade (76%), use of the sunscreen (68%), use of long-sleeved shirts (65 %); and the least used is umbrella (2%). On the other hand, 60% of respondents are parents, who were able to express that they are more careful with children in respect of sun protection. All of them protected their children by demanding the use of caps, and 80% demanded the use of sunscreens (see Fig 12, right). A total of 16% of respondents were exposed to the sun at these times without any protection, 62% rarely avoid it, and only 22% avoided to stay in the sun (Fig. 13).

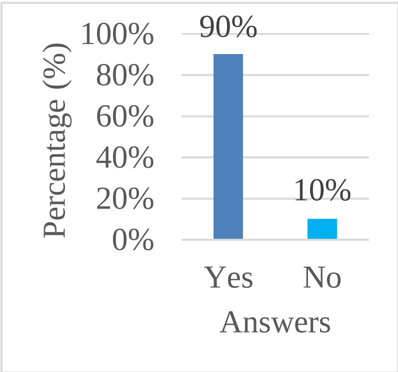

Figure 11. Percentage of people who protected themselves from the sun. Source: Prepared by authors.

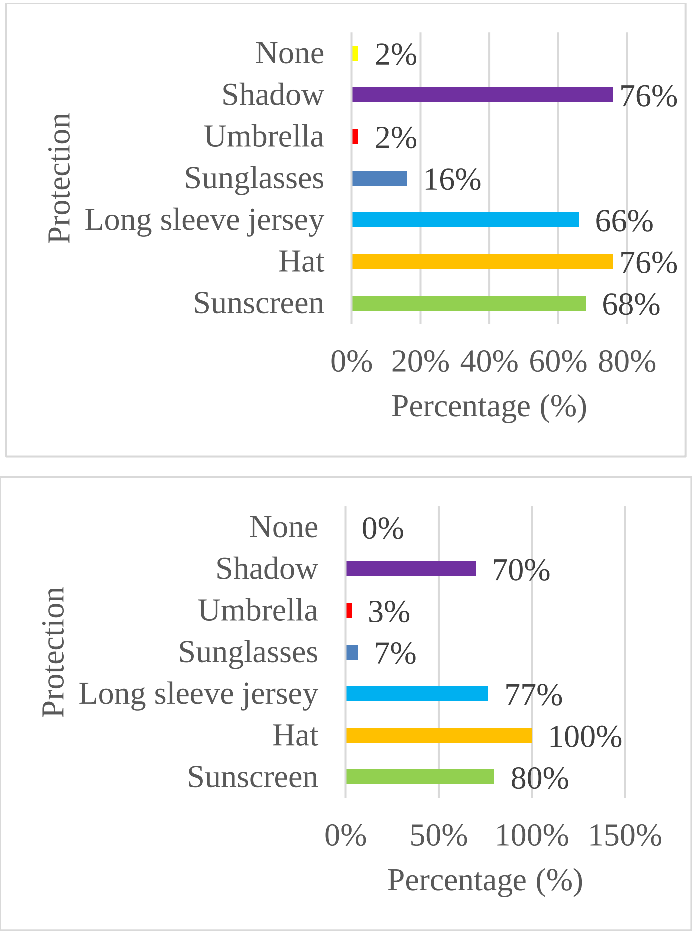

Figure 12. Survey about means for sun protection in adults (top) and children (bottom). Source: Prepared by authors.

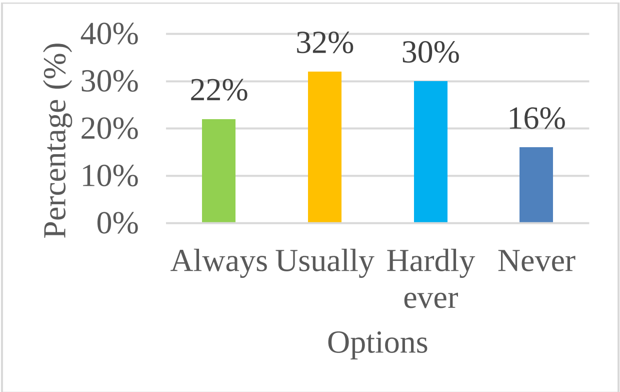

Figure 13. Frequency of sun-exposure avoidance between 11 to 14 hours. Source: Prepared by authors.

Despite the knowledge of the responders about the skin damage caused by solar radiation, they did not sufficiently observe protective measures in everyday life, some showing a slight burn. For instance, most of the responders did not know that sunscreen should be applied every two hours.

With respect to the frequency the responders sought for dermatological advice, 84% of the respondents had never seen a dermatologist (Fig. 14). Also, only 54% took care about any abnormality in the skin, such as the size, texture, color, and shape change of the moles (Fig 15.)

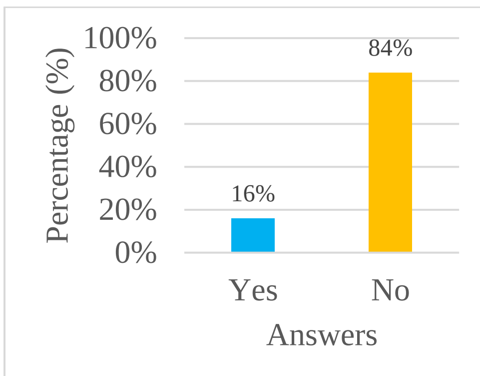

Figure 14. Percentages of people who paid a visit to the dermatology office. Source: Prepared by authors.

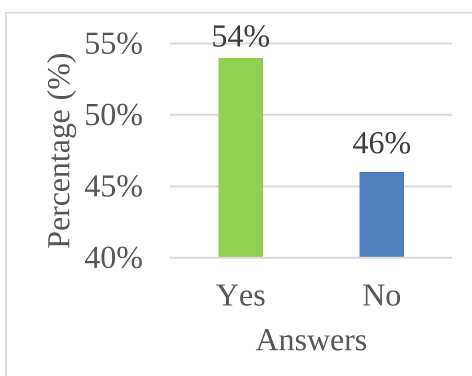

Figure 15. Percentages of people who paid attention to moles and skin spots. Source: Prepared by authors.

On the other hand, to know if people would use an application for the prognosis of skin cancer, we proceeded to ask in the surveys. And it was obtained that 76% are interested in this application, and 24% disagree (Fig. 16). This minority percentage is because people are not related to technology; many of them were older adults.

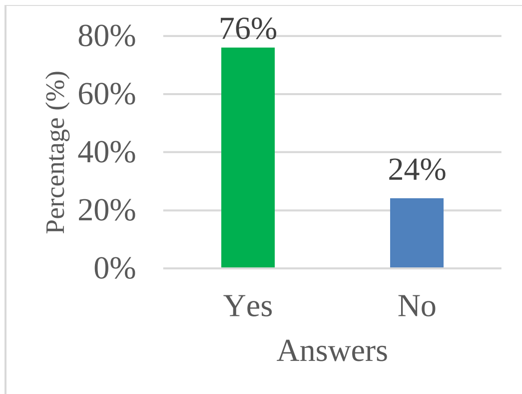

Figure 16. People interest in using an application that examines skin spots by photographs to prevent skin cancer. Source: Prepared by authors.

Most people did not take a dermatology check due they could not cover the medical services. Besides, 16% of the people visited the dermatologist because a problem with acne (Fig. 14). For this reason, we have provided information about how they can examine the skin on its own, looking for abnormalities in its shape, color, and edges. Also, there was talk about the ABCDE rule that dermatologists use to detect melanoma skin cancer. Besides, we comment that the prompt medical intervention in the event of an abnormality in the skin can be of great help in reducing the risk of death from skin cancer. Thanks to these talks, we encouraged curiosity in the subject, and they learned the importance of visiting a dermatologist. Finally, a brochure provided by the Center for Comprehensive Dermatological Care (Cadermint SA) related to skin cancer and prevention was shared with the surveyed people. This is of great importance to this group of people since they are all day under solar radiation due to work.

3 Solar radiation as main factor for developing skin cancer

3.1 UV Radiation

Ultraviolet (UV) radiation, that reaches the Earth surface, covers a range from 290 to 400 nm, and it is divided into three types UVA, UVB and UVC (5). The wavelengths of UV radiation that reach the Earth's surface are UVA (320-400 nm) and UVB (290-320 nm), with UVB being the most harmful and related to the increasing incidence of skin cancer (41).

The skin undergoing a chronic exposure of UV radiation induces biological responses, for example: skin burn, edema, erythema, immunosuppression, photoaging, DNA damage (41). The skin burn is due to the excess of UVB, which leads to different types of skin cancer through the generation of molecules such as hydroxyl radicals and oxygen. The photo-energy emitted by solar radiation triggers a cascade of biochemical events causing subsequent changes in the cell. Consequently, these photons directly damage DNA nucleic acids and proteins, accelerating skin aging and can lead to cancer formation (6).

3.2 UV radiation in Ecuador

Regions near the equator line have a UV index greater than 11. The UV index is the average effective UV irradiance in W / m2 multiplied by 40 [m2 / W] that shows the levels of ultraviolet radiation that reaches the surface of the earth (42),(7). According to studies carried out by Huaca et al. (7) explain the city of Ibarra in Ecuador have UV index values higher than 11 (low limit of “extreme UVI”) in 72 days of 82 days measured; and in 14 days it reached values higher than 20(extremely high), reaching a maximum value greater than 22 (0.55W / m^2).

3.3 Factors affecting UV radiation

3.3.1 Albedo

It is the reflectivity of a surface to solar irradiation, this varies with the wavelength of emitted radiation (43). Albedo varies depending on the season, type of surface, and angle of solar incidence (44).

Figure 17 shows a picture of global albedo from the measuring instrument MODIS (Moderate Resolution Imaging Spectroradiometer) aboard to the Terra/NASA satellite. This image was obtained from a composition of images in the period from April 7th to April 22nd of 2002.

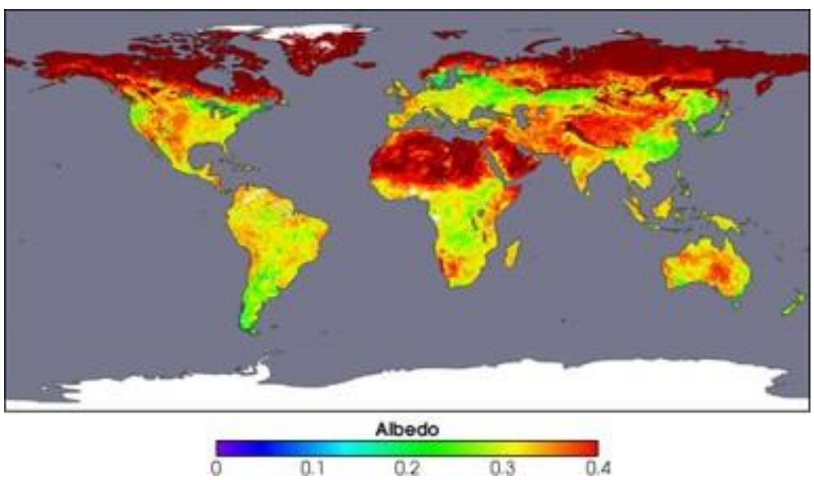

Figure 17. Global albedo from the measuring instrument MODIS aboard to the Terra/NASA satellite *(45)*.

In Ecuador, the value of albedo varies according to its regions. According to NASA POWER (Prediction of Worldwide Energy Resource) Project of NASA (46), the Ecuadorian coastal area has an albedo that varies monthly between 0.14-0.17, and the Andean region has an albedo that varies between 0.18 and 0.22. A low albedo heats the neighborhood because most of the light is absorbed by it, which happens in the coastal region.

3.3.2 Aerosol

Aerosol is a particle, solid or liquid, colloidal in suspension in the earth's atmosphere. Some organic aerosol particles disperse solar radiation into space and can cool the Earth's surface (47)(48). The gases and aerosols that make up the atmosphere absorb solar energy and scatter the radiation in certain bands of the spectrum. In other words, the presence of aerosols reduces direct solar radiation (49).

The parameter that represents the concentration of atmospheric aerosols in the air column above our heads is the *AOD_{550nm}, the aerosol optical depth at 550 nm.* In other words, AOD_{550nm} is a measure of aerosol charge that depends on the composition, size, and amount of aerosol particles present in the atmosphere. These measurements vary with radiation lengths.

3.3.3 Total Ozone Column

Ozone is colorless and odorless gas of low molecular weight, formed by three oxygen atoms (50). Ultraviolet, visible, and near-infrared radiations are absorbed by ozone before reaching Earth. Ozone has a very strong absorption band (visible region of 0.45 to 0.77 um), strong (0.2 to 0.3 um) and weak (0.3 to 0.35 um). Therefore, the ozone layer filters most of the ultraviolet radiation (51).

3.4 Solar irradiance and its DNA damage effect

3.4.1 Solar spectral UV irradiance

The spectral solar irradiance is the entry of radiant energy within a wavelength range. Its units are $Wm^{-2}(nm)^{-1}$ (52). The subtle changes in irradiance can have a dramatic impact on the Earth's climate, atmosphere, and ionosphere (53). Also, knowledge of the spectral irradiance that reaches the surface of the earth is essential in determining whether such radiation alters the biological action (54).

The American Society for Testing and Materials (ASTM), photovoltaic industry, and government laboratories (55) developed the normal and total global spectral irradiance standard reference. The ASTM spectra details the terrestrial solar spectral irradiance on the inclined surface facing the sun at 37 ° under a set of specific atmospheric conditions. These conditions are turbidity, presence of suspended particles in water, at 500 nm; the total column of water vapor at 1.42 cm; the total ozone content equivalent to 0.34 cm and albedo. The spectra are modelling using the simple SMARTS2 model, and the standard reference spectra graphs show in the figure 18.

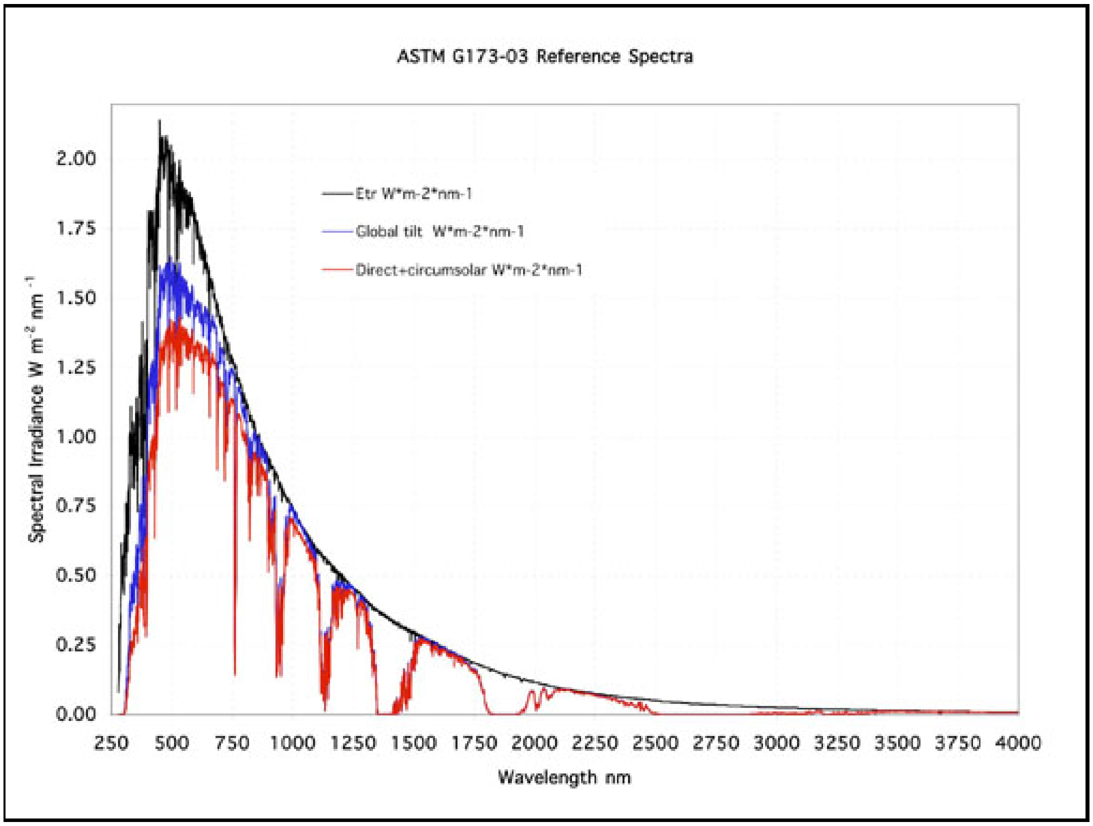

Figure 18. Direct Normal Spectral Irradiance, and the Global Total Spectral Irradiance on the 37° sun facing tilted surface for the atmospheric conditions *(55)*.

3.4.2 Modelling UV irradiance: SMARTS model

SMARTS is a model that predicts direct, diffuse, and global spectral surface radiation from 280 to 4000 nm, wavelengths that encompass UV, visible, and near infrared.

This model was developed by Dr. Christian Gueymard and written in FORTRAN code. To calculate surface radiation is essential to implement this spectral model in areas of clear sky (sky with cloudiness less than 25%). Furthermore, solar spectral irradiance is calculated from environmental parameters such as total ozone column, aerosol, the total column of precipitable water, albedo, relative humidity at 2 meters, the temperature at 2 meters, and carbon dioxide; also, information about the place such as latitude, longitude, and from to weather station. All these parameters must be introduced to achieve a better computational prediction of solar irradiance (56). Figure 19 shows the parameters that are introduced in the SMARTS for modelling UV irradiance.

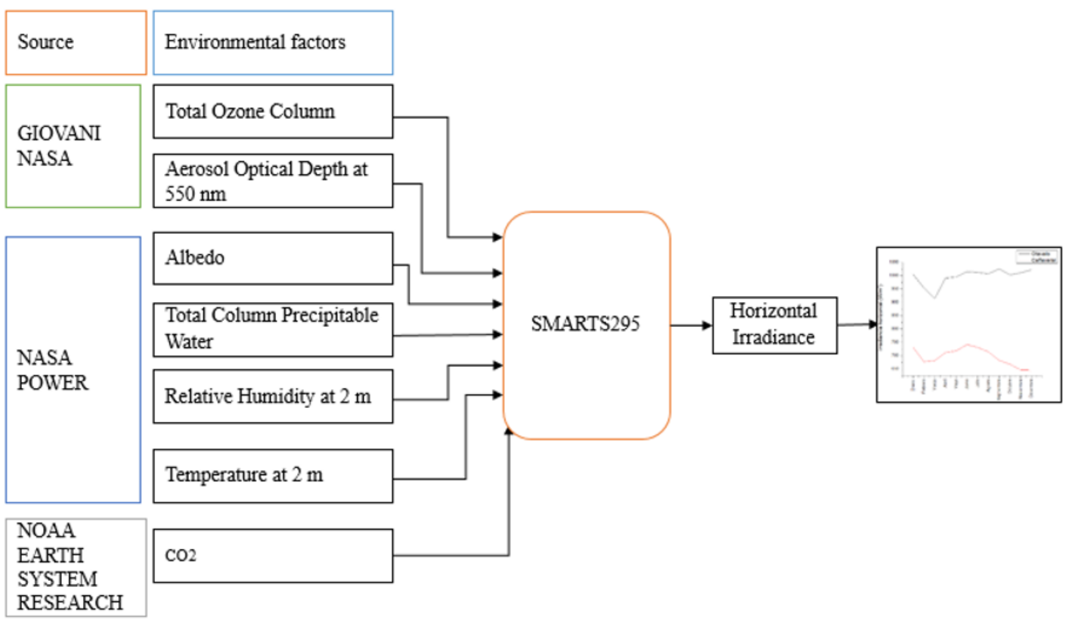

Figure 19. Diagram of the methodology to execute SMARTS software. Source: Prepared by authors.

3.4.3 Action Spectrum of DNA damage

An action spectrum (relative effectiveness [1/(UV dose) cm^2mJ^{-1}] as a function of wavelength) is a graph that shows the efficiency with which radiation produces a biological response that might to affects at a molecular level, such as DNA damage (Fig. 20). "Relative effectiveness" may refer to produce a biological effect as compared to UV radiation (57). The action spectra for melanogenesis on white skin are determined for wavelengths between 250 and 435 nm (58). Also, action spectra are vitally crucial in predicting the skin's response to ultraviolet radiation (59).

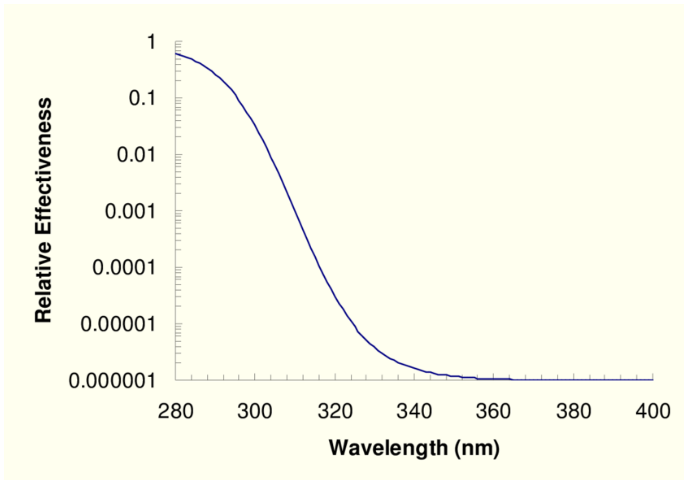

Figure 20. Action spectrum of DNA damage *(59)* from Setlow (1974).

3.5 Methodology of modeling UV radiation

For the study of UV radiation modeling in Otavalo and Cañaveral, carry out an exploratory and correlational investigation because, in the first instance, there is no background on the proposed topic. Likewise, the obtained solar radiation data is analyzed with the damages that this produces to the skin. Besides, this study looks at the relationship of solar radiation with environmental factors.

To stablish a relationship between the skin cancer and solar radiation, we analyzed the spectral solar irradiance in a horizontal plane as modeled in the cities of Otavalo (0.234 ° N, 78.262 ° W 2532 m.a.s.l) and Cañaveral (0.217 ° N, 80.033 ° W, 52 m.a.s.l.), located in the Andean nd Ecuadorian Coast regions respectively. In order to calculate the solar spectral horizontal irradiance, the values of environmental atmospheric and meteorological factors (Total Ozone Colum, AOD_{550nm},, Albedo,Precipitable Water, Relative Humidity at 2m, Temperature at 2 m, CO_2) in Otavalo and Cañaveral (Fig.14) were obtained from three different databases: Giovani/NASA, Power/NASA, and NOAA Earth System Research. These web pages are tool that provides us with large amounts of satellite scientific data to analyze and visualize without having to download original data (60). Then, environmental factors data from 2010 to 2018 were averaged in a monthly basis, and along with the following variables: solar constant, latitude, longitude, altitude, and time of year, they were computed by the SMARTS model. With above, horizontal solar spectral irradiance, as a function of the wavelength in the range of 280 to 400 nm, was obtained for each month at noon in both cities.

Then, with the collected data (shown in Table 2 and Table 3), the putative DNA damage was associated with the reckoned radiation dose. For that, the action spectrum of DNA damage (Fig 20) was normalized and then multiplied with the irradiance spectrum of each month. Next, this product was integrated to find the effective irradiance of DNA damage. Finally, the data of horizontal irradiance, effective irradiance of DNA damage, Total Ozone Column, and Aerosol Optical Depth at 550 nm were plotted according to the months of the year for each city.

3.6 Results and discussion

Before modeling, we proceed to analyze some factors, such as the AOD at 550 nm.. The data of the seven parameters for modeling UV radiation in the range of 320 to 400 nm with the SMARTS model, is shown in the Tables 2 and 3.

Table 2. Data of the seven environmental factors of the city of Otavalo. Source: Prepared by authors.

Month	Temperature (°C)	Relative humidity (%)	Total Column Precipitable Water (mm)	Ozone Total Column (cm)	CO2 (ppm)	Aerosol Optical Depth 550 nm	Albedo (dimensionless)
January	13.30	84.73	5.36	0.24	358.36	0.05	0.19
February	13.36	85.27	5.48	0.24	398.88	0.10	0.18
March	13.49	84.97	5.51	0.25	399.82	0.13	0.17
April	13.50	85.27	5.66	0.25	401.3	0.06	0.17
May	13.33	85.20	5.58	0.24	402.01	0.06	0.17
June	12.46	82.95	5.33	0.25	401.2	0.05	0.18
July	12.29	81.35	5.08	0.26	399.45	0.06	0.17
August	12.48	78.68	4.98	0.26	397.38	0.06	0.17
September	12.85	77.45	5.11	0.27	395.94	0.04	0.19
October	13.30	80.76	5.04	0.26	396.28	0.06	0.17
November	13.31	83.34	5.01	0.25	397.91	0.05	0.18
December	13.17	83.90	5.21	0.24	399.32	0.04	0.19

Table 3. Data of the seven environmental factors of Cañaveral city. Source: Prepared by authors.

Month	Temperature (°C)	Relative humidity (%)	Total Column Precipitable Water (mm)	Ozone Total Column (cm)	CO2 (ppm)	Aerosol Optical Depth 550 nm	Albedo (dimensionless)
January	25.30	84.32	5.36	0.24	358.36	0.25	0.06
February	25.52	85.37	5.48	0.24	398.88	0.31	0.05
March	25.77	85.26	5.51	0.25	399.82	0.31	0.05
April	25.72	85.93	5.66	0.25	401.3	0.27	0.06
May	25.47	85.63	5.58	0.25	402.01	0.26	0.06
June	25.05	84.61	5.33	0.25	401.2	0.24	0.06
July	24.73	82.71	5.08	0.26	399.45	0.26	0.06
August	24.60	80.08	4.98	0.27	397.38	0.29	0.07
September	24.81	78.39	5.11	0.27	395.94	0.33	0.07
October	24.67	77.95	5.04	0.27	396.28	0.35	0.06
November	24.59	78.06	5.01	0.26	397.91	0.38	0.06
December	25.02	80.16	5.21	0.25	399.32	0.37	0.06

Figure 21 (left) shows the annual evolution of monthly averaged values of AOD_{550nm} in the period of 2010-2018. In Cañaveral, it was presented maximum AOD at 550nm value of 0.38 and 0.24 in November and June, respectively. As to Otavalo, there was a maximum of 0.13 in March, and of 0.10 in February. Both cities presented the highest concentration of aerosols in February. AOD_{550nm} values in Cañaveral were higher than Otavalo.

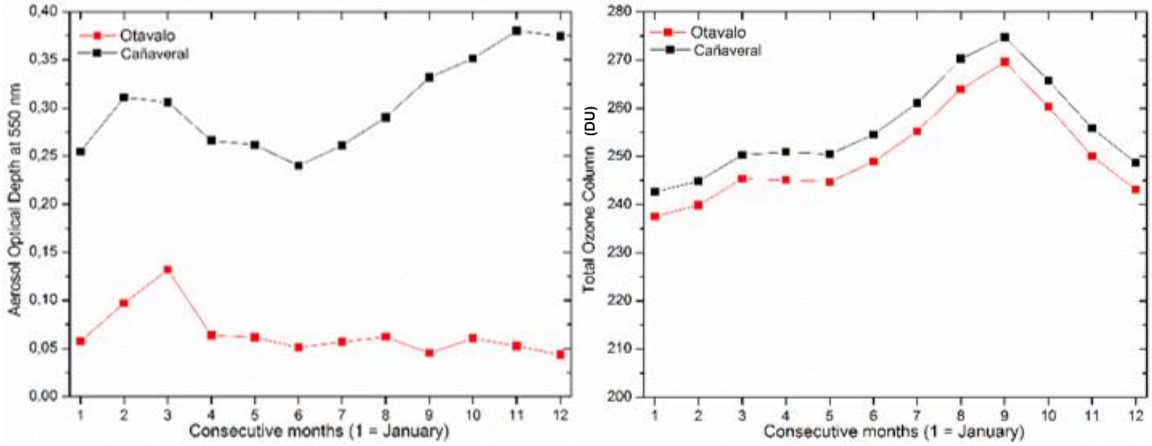

Figure 21. Monthly averages of AOD (Optical depth of aerosols) at 550 nm (left) and total ozone column (right) in Dobson units (DU) in Cañaveral (black) and in Otavalo (red) from 2010 to 2018. Source: Prepared by authors.

Total column ozone refers to how many ozone molecules are in the air and this amount is expressed in Dobson units. Besides, ozone absorbs UVB radiation as it passes through the atmosphere (61) (62). Figure 21 (right) shows the total ozone columns in the two cities Otavalo and Cañaveral, we obtained (256±10) cm for Cañaveral and (250±10) Dobson units for Otavalo. The annual evolution of the ozone, and in both cities the maximum values are produced in September. Also, during the entire year, Cañaveral had a higher concentration of ozone molecules that Otavalo. With this result, it could be said that Cañaveral had lower radiation than Otavalo since most of UVB radiation was absorbed by ozone.

The modelling of UV radiation carried out in both cities with the SMARTS295 program. SMARTS295 (Simple Model of the Atmospheric Radiative Transfer of Sunshine) is a simple dispersion model that predicts direct, diffuse and global solar radiation that covers the range of 280 to 4000 nm; including UVA, UVB, visible spectrum and near-infrared bands (63). This model was created by Gueymard (1995).

To perform the modeling of UV radiation, we chose the spectrum of the range of 280 to 400 nm, which covers ultraviolet A and B rays. This selection was made according to the recommendations of the American Cancer Society (64), which states that both UVA and UVB rays can damage the skin and increase the risk of skin cancer. UVA is the radiation that mainly reaches the surface of the earth and is the cause of skin aging and long-term DNA damage. UVB reaches the surface a minimum percentage since it is partially absorbed by ozone. However, this radiation has more energy than UVA, so it can directly damage the DNA of the skin cells and is the cause of the redness. On the other hand, UVC rays have less energy, so it does not reach the surface since it is absorbed by oxygen and ozone from the atmosphere.

Figure 22 (left) shows the average monthly values of UV radiation from January 2010 to December 2018 in both cities. Cañaveral had a maximum UV radiation intensity in August (25 Wm^{-2}) and a minimum intensity in February (15 Wm^{-2}), while Otavalo showed low radiation in February (51 Wm^{-2}), and March (41 Wm^{-2}), and the rest of the months, it has a high presence of radiation that varies between 61 and 65 Wm^{-2}.

It can be noted that Otavalo has more solar radiation entering the surface of the Earth than Cañaveral. This likely occurred because Otavalo is located at more altitude. On the other hand, if the AOD_{550nm} and total ozone column with the horizontal irradiance are analyzed, it can be concluded that, there is an inversely proportional relationship. That is, as lower is the AOD_{550nm}, the higher the radiation, and as smaller the total column of the ozone, higher the radiation. Then, Otavalo has a lower concentration of AOD_{550nm} and ozone, so there is a more significant influx of UVA and UVB radiation to the earth's surface.

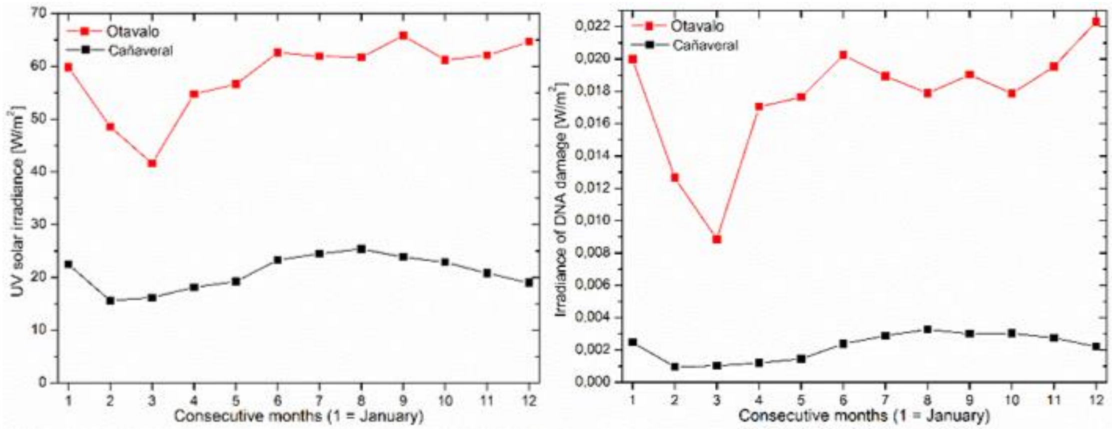

Figure 22. Monthly averages of solar irradiance (left) and Irradiance causing DNA damage (right) from 2010 to 2018 in Cañaveral (black) and Otavalo (red). Source: Prepared by authors.

Finally, Figure 22 (right) shows the monthly averaged values of the effective radiation that causes DNA damage. We can observe that Otavalo has much higher values of effective radiation than Cañaveral, which comprises between 0.009 and 0.022 Wm^{-2}, and Cañaveral has values between 0.001 and 0.003 $W\ m^{-2}$.

UV radiation has a mutagenic effect on certain biological molecules depending on the wavelength (65). According to the spectrum of action to damage DNA (see figure 20), the DNA has an energy absorption peak at 260 nm; this energy is reduced down to zero energy at 400 nm (wavelengths that cover UVA and UVB). The absorbed energy triggers a series of biochemical reactions in the cell to provoke structural damage to the DNA. It is believed that these changes are responsible for inducing skin cancer (6). Interestingly, it was observed the same pattern between solar irradiance and irradiance of DNA damage (see fig 22), which suggested that there was a correlation between the energy emitted by UV radiation and photolesions in skin cells. Finally, the result obtained shows that in Otavalo, the risk of getting DNA damage was greater than in Cañaveral, this predisposing people from later city to develop skin cancer. Besides, some studies also show that DNA damage is one of the factors related to skin cancer due to prolonged exposures (5)(14).

4 Software for prognosis of skin cancer

This chapter will discuss basic concepts necessary to understand the following objective of the thesis, which are the design of automatic software for the previous diagnosis of skin cancer using images and a simple convolutional neural network.

4.1 Mathematical model of an image

A digital image is a matrix array of dots (x, y) that represents the intensity of the color (pixel) in that position. Then we can see an image as a function f (x, y)(66). For instance, the binary image (on the left of Fig. 23) can be represented by a 5x5 matrix (on the right) whose elements are the values 0 and 1, which represents black and white pixels, respectively.

$$\begin{matrix} 1&1&1&1&1 \\ 1&0&0&0&1 \\ 1&0&1&0&1 \\ 1&0&0&0&1 \\ 1&1&1&1&1 \end{matrix}$$

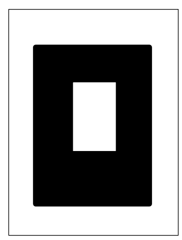

Figure 23. Matrix 5x5 (left) with its respective image (right)

On the other hand, color images have independent matrices that each of these specifies the intensity of each color. In the case of the RGB model, there are 3 arrays. These arrays are red, green, and blue. RGB combines these three colors obtaining almost all visible colors. RGB is used for processing and storage of digital images. However, RGB is not a favorable option when luminance and chrominance data are mixing (67).

4.2 Preprocessing an image

The image preprocessing is a critical step in image diagnosis, which is aimed to improve the quality of the original image. Preprocessing uses algorithms to correct image flaws like illumination, and filters to reduce background noise and artifacts. For example, Gamma correction is a method for lighting correction (68); and Gaussian, median, and anisotropic are filters for reducing noise in an image (39).

4.3 Learning and classification

Image recognition is a relatively simple task for humans, but it is a difficult task for computers. This is because biological systems have a different architecture from that of a computer. For this reason, there are new computer models that try to simulate some characteristics of the human brain to create patterns, recognize information, or solve problems (69).

4.3.1 Artificial intelligence

Artificial Intelligence (AI) is the combination of algorithms that aims at faster processing of information than a human brain. AI has recently shown superior performance in several domains; one of them is medicine. For example, AI is being applied in the analysis of images in dermatology. In this area, AI helps to better prevention, detection, timely diagnosis for the treatment of skin cancer. While the diagnostic system never reaches 100%, doctors reliably improve system performance. AI encompasses Machine Learning and Deep Learning (70) (71) (72).

4.3.1.1 Machine learning

A machine learning system is a set of techniques that aim to "learn" from the data and then recognize the situation or make predictions about them. Therefore, this system must have a training process (73).

4.3.1.2 Deep learning

Deep learning is a specific sub-field of Machine Learning discipline, which uses deep neural networks (see below). The deep term represents the idea of successive and hierarchical data through layers (69)(74)

4.3.1.3 Neural network

A neural network is a set of artificial neurons connected between them that transmit a signal. It tries to create mathematical models to solve problems using conventional algorithmic techniques. The neural network simulates some tasks performed by the human brain such as image recognition (75).

4.3.2 Biological neural networks vs artificial neural networks

The neuron is the basic computational unit of the brain. It has approximately 86 billion neurons in the human nervous system and is connected by synapses. Each neuron receives an input signal from its dendrites and produces an output signal along the axon. The axon branches and connects with dendrites of other neurons through synapses. Likewise, in the computational model of a neuron, the signal enters from a terminal axon of a neuron (Xo). And upon contact with the dendrite of another neuron depending on the synaptic force (WoXo), the signal travels along the axon applying the activation function or non-linearity (See figure 24). Then the output of this model will be given by the following equation (76):

$$y(x, w) = f\left(\sum_{i=0}^{2} x_i w_i + b\right)$$

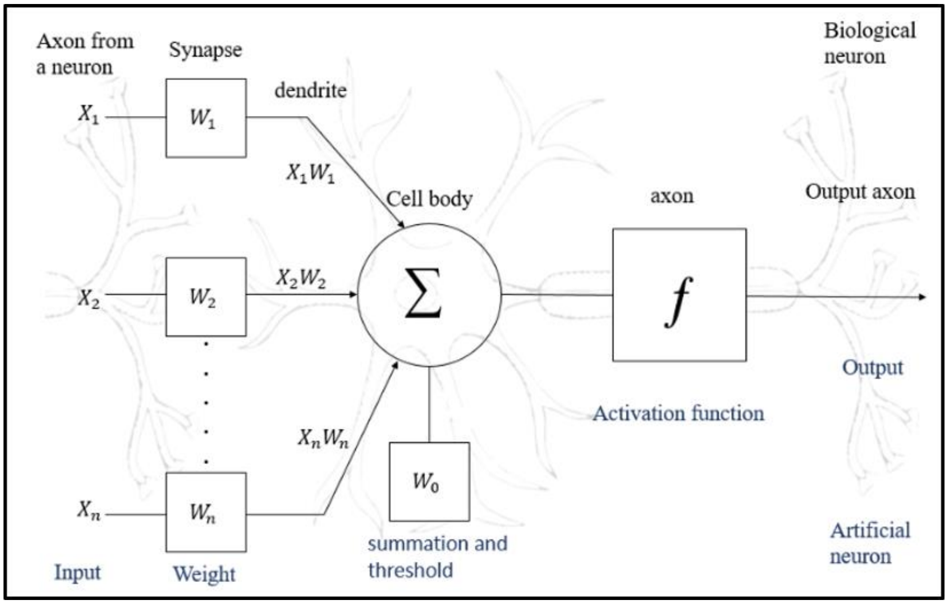

Figure 24. Structure of a biological neuron and an artificial neuron using a mathematical model. Image adapted from Requena et al. *(77)*.

4.3.3 Convolutional neural networks (CNN)

CNNs are a specific type of neural network that implies the use of convolution, a mathematical operation, in their hidden layers. It is useful for an image-focused task like object detection and image classification (78) (35).

4.3.3.1 CNN architecture

CNNs consist of convolutional layers, subsampling layers, and fully connected layers. These layers can be stacked in different ways, resulting in different CNN architectures (79)(80). A simple CNN architecture is illustrated in figure 25.

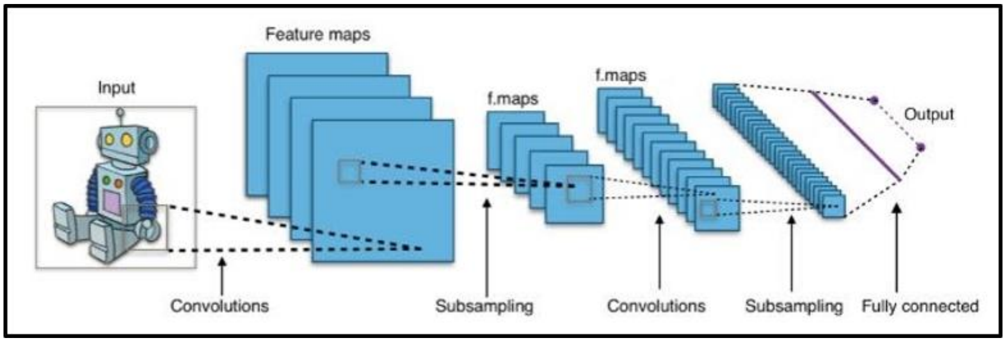

Figure 25. A simple CNN architecture *(81)*.

4.3.3.2 Convolutional layer

In this layer, convolution operation is performed between the image matrix (I) and a small matrix called kernel or filter (K) to extract features like edges (Fig. 26). The center element of the kernel is placed over the source pixel, then calculation by elements in the input matrix performed and replaced with a weighted sum of itself and any nearby pixels (79). The kernel moves through the image matrix with a certain stride value. The kernel moves to the right until the width completed. Then it hops down to the left of the image with the same stride value. This process occurs until the entire image traversed, resulting in a new matrix (79)(78).

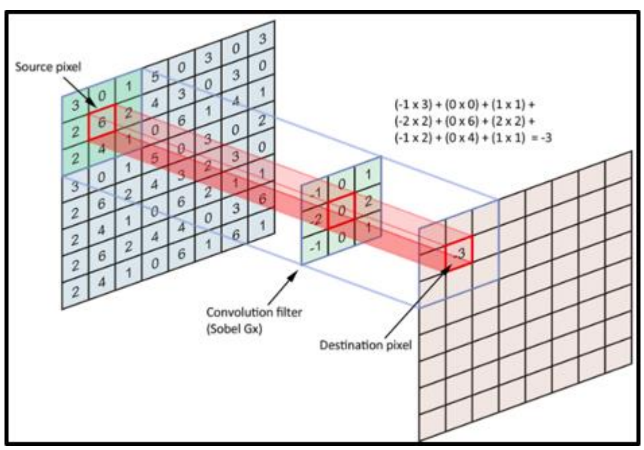

Figure 26. Convolutional operation *(82)*

4.3.3.3 Subsampling or Pooling layer

In this layer, the size of the matrix reduces before entering to new convolutional layer to avoid an excessive number of neurons and decrease the computing power required to process the data. The pooling could be Max Pooling, returns the higher value, and Average Pooling returns the average of the values (78)(79). To do this, a size of pooling (a submatrix) defines, and only one value is obtained from the portion of the image matrix covered by it, as shown in figure 27.

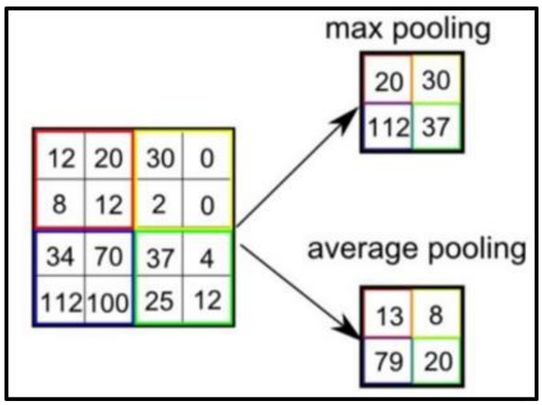

Figure 27. An illustrative example of pooling´s types with 2x2 filter and stride 2 *(83)*.

4.3.3.4 Fully connected layer

This layer receives high-level filtered images and classifies them (80).

4.4 Methodology of Software development

For software development, an exploratory investigation was carried out to gather information about the use of the CNN proposed for classification of the four classes chosen -benign, melanoma, basal and squamous cell carcinomas- to establish proposals for future research based on the quantitative data obtained.

4.4.1 Hardware and Software

The program has been executed on a computer with Intel(R) Core(TM) i5-6200U CPU processor, and 8 GB RAM. For the program to work properly it was necessary to have Python 3.7.4 and the respective libraries including Opencv, Numpy, and tf.Keras, which are explained below.

- *OpenCV* (Open source Computer Vision) is a library to image processing and computer vision tasks (84).
- *NumPy* (Numerical Python) is a library to numerical tasks as manipulating matrices (84).
- *tf.Keras* is Keras functional API in TensorFlow to build and train deep learning models (85).

4.4.2 Dataset

A dataset did collect RGB skin images in the JPG format of four classes-benign, basal cell carcinoma, melanoma, and squamous cell carcinoma. The images were obtained from the International Skin Imaging (ISIC) database and also were provided by Dr. Cecilia Cañarte of the Center for Dermatological Integral Cadermint SA. ISIC database consists of 2169 images of melanoma cancer, 19373 images of benign, 625 images of BCC and only 250 SCC images which makes the dataset unbalanced. Also, it consists mainly of dermatological images and only 100 clinics images. Dr. Cecilia Cañarte provided 29 clinical images divided into 3 melanomas, 9 BCC, and 17 SCC. Due to the scarcity of clinical images from both sources, these augmented with the cropping method. The cropping method consists of making different cuts to the same image. Then, the dataset reduced considering the resolution of the image and its detail to obtain a balanced dataset. Finally, the dataset consists of 1000 skin images of moles and spots correspond to the four classes with 250 images for each category. A summary of available data can see in Table 4 and a image of each type is found in the figure 28.

Table 4. Dataset composition. Source: Prepared by authors.

Lesion type	Dermatological images	Clinical images	Total images
Melanoma	190	60	250

Benign	250	0	250
Basal cell carcinoma	204	46	250
Squamous	210	40	250
Total images	854	146	1000

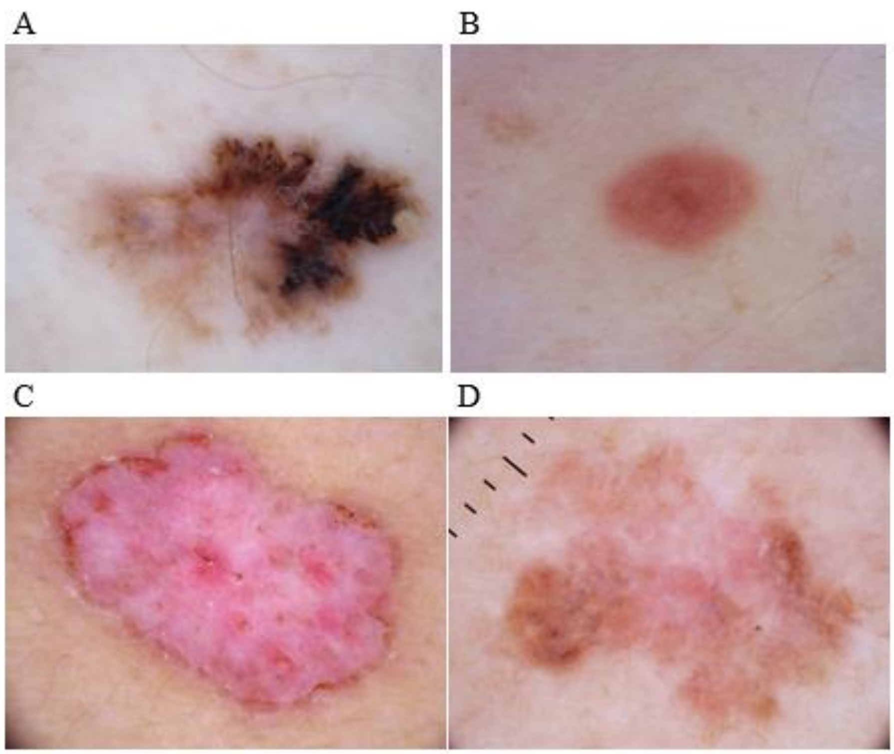

Figure 28 . Example of the dataset images. A) Melanoma B) Benign C) Basal D) Squamous. Source: Prepared by authors.

Then, the image processing commands of the Opencv library reviewed, as well as the neural network commands of the Keras library, and some codes that were very helpful for the software development. The software implementation was done entirely in the Python ® programming language because its amenability and open source.

The proposed skin cancer detection method was divided into two parts: image preprocessing, and the CNN model (see Fig 29). CNN was chosen since it automatically identifies the important features of a picture without any human supervision. Besides, it is excellent for reducing the complexity of the model without losing its quality. Consequently, it has faster training and reduces the chance of overfitting than other types of neural networks when working with images (86).

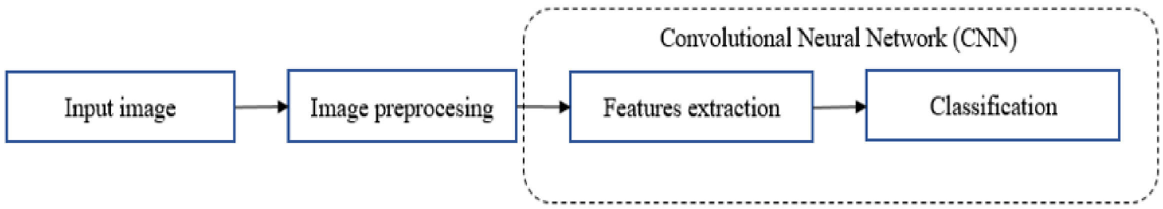

Figure 29. Skin Cancer detection system. Source: Prepared by authors.

4.4.3 Image Preprocessing

In order to improve the images some commands from the OpenCV library were used like cv2.imread to load the image, cv2.bilateralFilter to apply the bilateral filter to reduce noise, and cv2.resize to adjust the image size to 200 x 200 pixels due to the images exhibited random dimensions. Besides, a gamma correction algorithm found on pyimagesearch made by Rosebrock (87) was used to correct lighting artifacts. The code founds in Annex 3. Part A

4.4.4 Feature extraction and classification

The proposed software uses a Convolutional Neural Network or CNN to the automatic feature extraction and classification of the skin images. It was programmed using the Keras functional API in TensorFlow.

4.4.5 CNN architecture

The CNN architecture was obtained by modifying a code derived from GitHub repository (88). The final CNN architecture is shown in the Figure 30. It consists of five convolutional layers with a 3 x 3 kernel and an activation function ReLU (Rectified Linear Unit). There were 32 feature maps in the first convolutional layer, 64 features maps in the second convolutional layer, and 128 features maps in the rest. After each convolutional layer, there was one Max pooling layer 2x2. Also, there was a flatten layer which flattens the input without affecting the batch size (89). Besides, there was a 1-layer fully connected of 300 neurons with activation function ReLU followed by a dropout with a probability of 0.5. Finally, a 1-layer fully connected of 4 neurons receives the output and classifies them using the activation function Softmax (90).

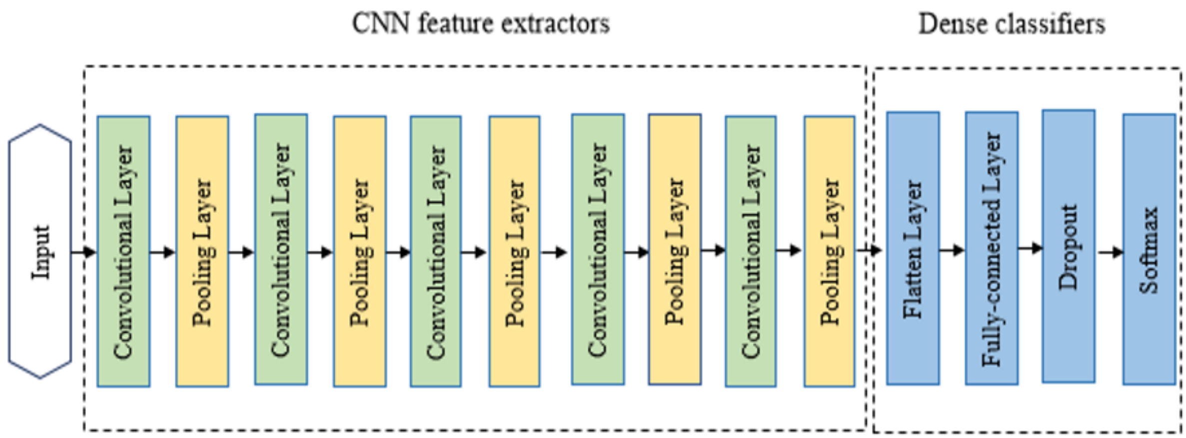

Figure 30. CNN architecture. Source: Prepared by authors.

4.4.6 Labeling stage

The labeling process consists of pointing to the neural network, the different classes that exist. The preprocessed images were not labeled manually, one by one, as melanoma, benign, SCC or BCC. It is because Keras library allows save the data in subdirectories and automatically generate tags using flow from directory, which is a method that identify classes automatically from the folder name (91).

4.4.7 Training, Validation, and Testing

Before feeding to the network, the dataset of 1000 images was divided into three randomly groups - 80% (800 images) for training, 10% (100 images) for validation, and 10% (100 images) for a test. This ratio was chosen because it is a common split used when the total available data size is low (less than 100,000) (92). Besides, each group has a specific function to get the final CNN model. First, the training dataset teaches to the network model how each of the skin lesions we want to classify look. Second, the validation dataset, images that the neural network does not see as part of the training, is used to checking how the model has been trained in each epoch using metrics like accuracy, which can be obtained from this validation dataset. It is a guide to decide how to tune the algorithm's parameters before repeating the training process for another epoch. Third, the test dataset was reserved for a final test. It contains data that the model has never seen before during the training stage (neither as training data nor as validation data). In consequence, this dataset allows getting a more objective measure to the algorithm and evaluate if the proposed model generalizes correctly. Besides, before feeding the network, the values of the images of each group were normalized to improve the learning of the neuronal network. Thus, each value was divided into 255 because the colors of the pixels have values ranging from 0 to 255. Then, values between 0 and 1 obtained. Finally, the CNN model was saved for its quantitative evaluation. The code founds in Annex 3. Part B.

4.4.8 Model evaluation

The metrics explained below were used for the quantitative evaluation of CNN performance.

- **Confusion matrix –** It is a table layout used to visualize the performance of a classification model. It compares the actual class with a predicted class to evaluate if there is any misleading in the forecasting (Fig 31.). The confusion matrix has four parameters: True positive (TP), False positive (FP), true negative (TN) and false-negative (FN). The following metrics can be calculated using these parameters (93).

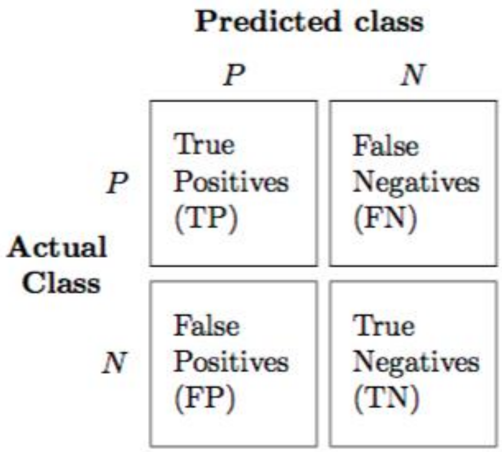

Figure 31. Confusion matrix for the Binary Classification *(94)*

- *Accuracy*. It is simply a ratio of correctly predicted observation to the total observations, regardless of the class (positive or negative) (93).

$$\text{Accuracy} = \frac{\text{TP} + \text{TN}}{\text{Total}}$$

- *Error rate*. It is the complement of accuracy (93).

$$\text{Error Rate} = \frac{\text{FP} + \text{FN}}{\text{Total}}$$

- *Precision.* It is the ratio of correctly predicted positive observations divided by the total predicted positive observations (93)

$$\text{Precision} = \frac{\text{TP}}{\text{TP} + \text{FP}}$$

- *Recall (sensitivity).* It measures the proportion of positives correctly identified as positive (95).

$$\text{Recall} = \frac{\text{TP}}{\text{TP} + \text{FN}}$$

- *Specificity.* It measures the proportion of negatives correctly identified as negative (95).

$$\text{Specificity} = \frac{\text{TN}}{\text{TN} + \text{FP}}$$

4.4.9 Graphical user interface (GUI)

The classification of a new image by the CNN model saved can do by a text terminal using the code founds in Annex 3. Part C. However, a graphical interface was created since it is more striking for a user to interact with a visual medium than with a text terminal.

For this, first, a brainstorm was performed to define the requirements of GUI and its content. Then, paper schemes were developed to have a clearer idea about the number of windows, buttons and determine the flow between them. Once the scheme was defined (Fig 32.), the graphic interface was created using the Tkinter, which is a standard Python package for creating graphical user interfaces (GUI) (96).

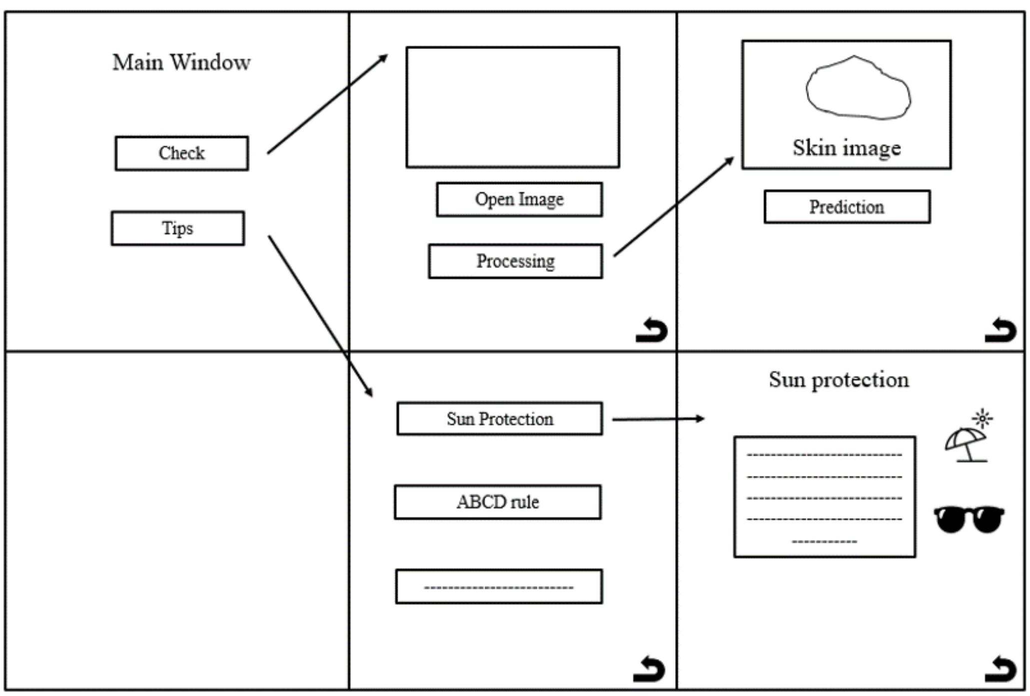

Figure 32. Scheme of GUI. Source: Prepared by authors.

4.5 Results and discussion

The proposed method consisted of two stages. First, it employed a preprocessing algorithm to reduce factors that could affect the convolutional neural network performance. In the second stage, the preprocessed images were fed into a CNN to features extraction and classification.

4.5.1 Preprocessing algorithm

Preprocessing algorithm is very significant because when working with skin images, there are some challenges. For example, the lesions to be analyzed have objects such as hairs and wrinkles that can mislead the neural network. Also, image quality depends on other factors, such as lighting. In this step, the gamma correction operation and bilateral filter have been proving with different values to find the values that give the best results for improving the quality of the images.

The figure 33 represent the skin cancer image after using gamma correction operation with gammas values 0.6, 1, 1.5 and 2. According to the images obtained, it was found that a gamma value of 1.5 is the most adequate for contrast and brightness because a gamma value of 0.6 shifts the image to the darkest side of the spectrum. This value increased the detail of the lesion, but also increased the details of hairs and wrinkles too. In contrast, and a gamma value of 2 shifts the image to the lighter end of the spectrum and lightening dark colors.

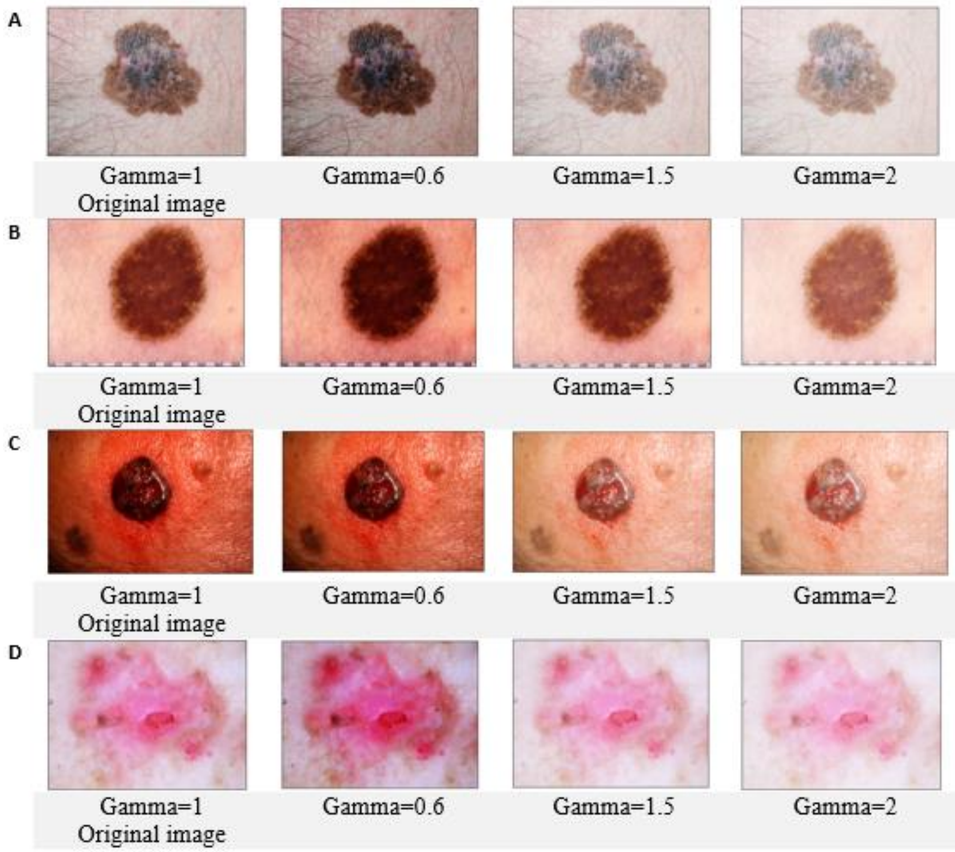

Figure 33. Result to different values of gamma correction operation to some images. A) Melanoma B) Benign C) Basal D) Squamous. Source: Prepared by authors.

Subsequently, a bilateral filter was applied. This filter was chosen because it helps to reduce noise (hair, wrinkles) by smoothing the image but keeps the edges (97). Setting a 3 x 3 bilateral filter with a sigma color of 25 and a sigma space of 75 gave the most adequate results after proving different values in each parameter.

Figure 34 shows the influence of the gamma correction operation and the bilateral filter on a melanoma image. The image B is a blurred image that keeps the edge of the lesion. In this way, certain artifacts like hairs are reducing, but the border that could be extracted by the convolutional layers of the CNN is maintained.

The final step of preprocessing consists to adjust the image size to 200 x 200 pixels to standardize the images and that the input of the convolutional neural network has the same size.

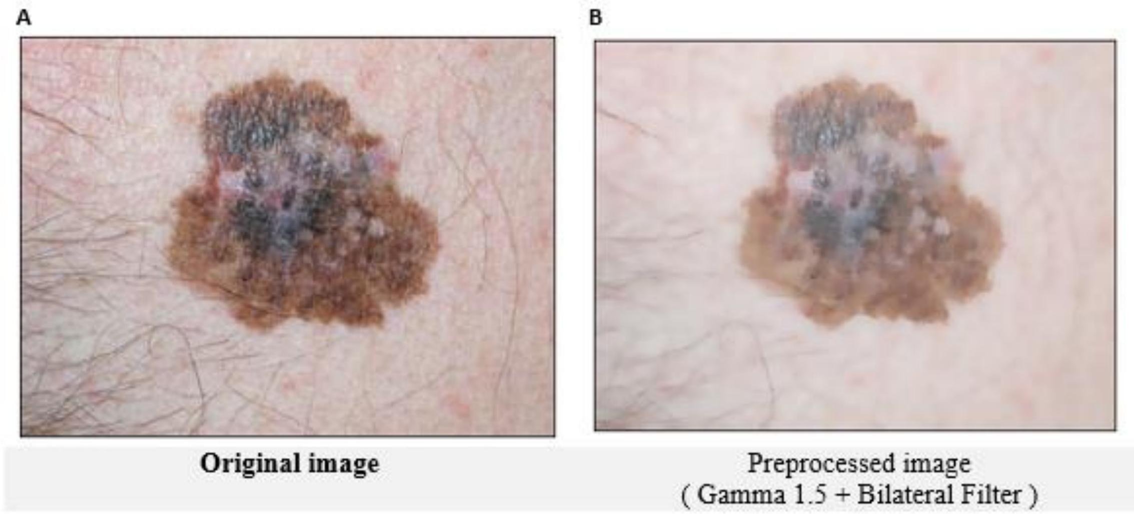

Figure 34. Original melanoma image in comparison with the preprocessed melanoma image with a gamma of 1.5 and a bilateral filter. Source: Prepared by authors.

4.5.2 CNN model

As mentioned before, the data was divided into three parts - training, validation, and testing. The three data sets were balanced. This is an important factor to ensure that the accuracy of the model can be an adequate metric to assess its validity. The data can see in Table 5.

Then of some tests performed by changing some hyperparameters of CNN like batch size, the number of epochs, and the learning rate, the hyperparameters for the learning process of the proposed model were the following. Since this is a multiclass classification problem and the final activation function is softmax, the model was trained with the loss function categorical cross-entropy or called softmax loss.

Table 5. Partition images for training, validation, and testing. Source: Prepared by authors.

Lesion type	Training	Validation	Test	Total
Melanoma	200	25	25	250
Benign	200	25	25	250
Basal cell carcinoma	200	25	25	250
Squamous	200	25	25	250
Total	800	100	100	1000

The Adam optimizer was used with a learning rate parameter of 0.00001, the number of epochs was 500, batch size of 10, and the accuracy metric had been chosen for monitoring the operation of the network. The network is trained through 10,000 iterations with a duration of 1 hour and 45 minutes. The number of iterations of our training is less than other works. For example, E. Nasr-Esfahani et al. (40) trained through 20,000 iterations and Mendes et al. (98) trained trough 38,000 iterations with a total time of 35 hours.

The accuracy and the loss curve for the testing and validation dataset of the final model are shown in figure 35 and figure 36, respectively.

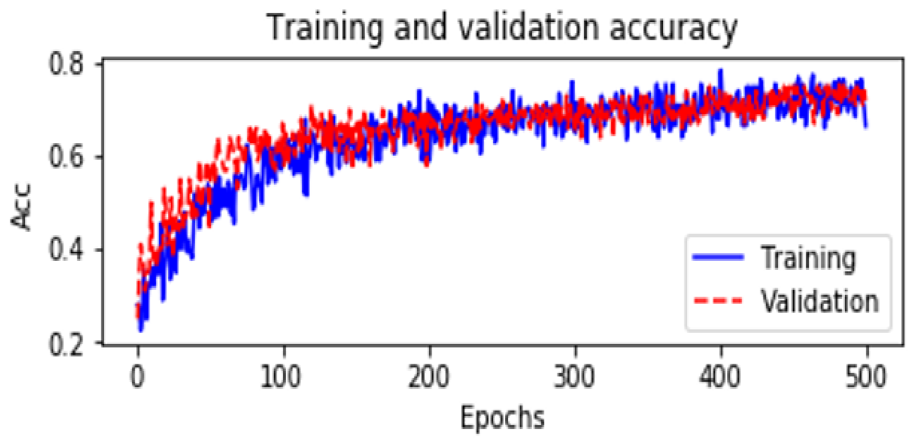

Figure 35. The training and validation loss. On the x-axis, the epochs are shown, on the y-axis the value of the loss function. The training curve shows in blue, and the dashed curve shown in red represent the validation. Source: Prepared by authors.

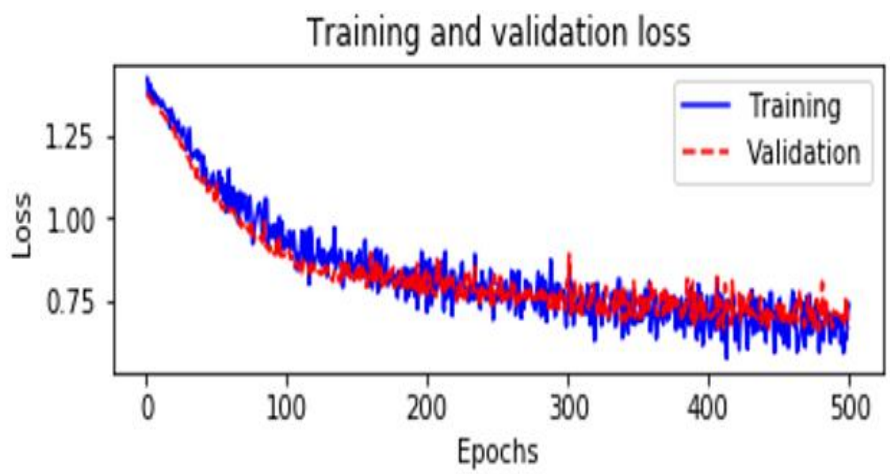

Figure 36. The training and validation accuracy. On the x-axis, the epochs are shown, on the y-axis the value of the accuracy. The training curve shows in blue, and the dashed curve shown in red represent the validation. Source: Prepared by authors.

For the loss function, a decrease is observed in each period for both training and validation, obtaining 0.67 and 0.68 in the last epoch, respectively. Also, for accuracy, an increase is observed for training and validation with each epoch, getting 0.71 and 0.74 in the last epoch, respectively.

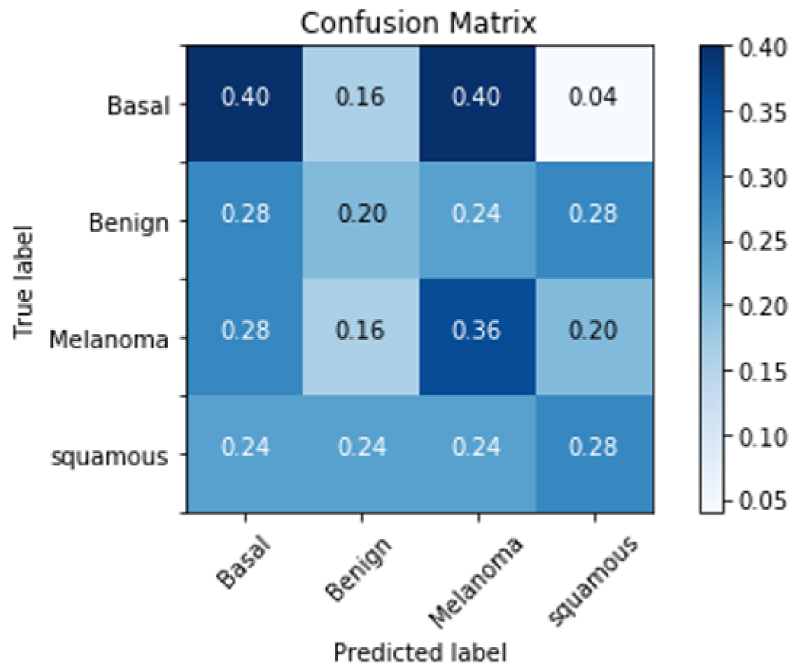

Figure 37. Normalized confusion matrix

Consequently, the behavior of the curves is as expected. Besides, no overfitting found. Therefore, the plots suggest that the model fits well with the problem. Then, we create an evaluation step, to check for the accuracy of our model training set versus the validation set. The confusion matrix obtained shows in figure 37.

As we can see in the confusion matrix generated for the predictions in the testing dataset, our machine is not pretty good at classifying which lesion is what. For example, Basal cell carcinomas (BCC) were misclassified as melanoma, and Benign were misclassified as Basal and squamous cell carcinoma. It most likely due to the many different types of patterns on each type of skin lesion. Finally, the table shows the metrics calculated from the confusion matrix, which will be analyzed to suggest future work that could improve network performance.

Table 6. Metrics calculated from the confusion matrix.

	Basal	Benign	Melanoma	Squamous	Average
Accuracy	0.65	0.66	0.62	0.69	0.66
Error rate	0.35	0.34	0.38	0.31	0.34
Precision	0.33	0.26	0.29	0.35	0.31
Recall (Sensitivity)	0.4	0.20	0.36	0.28	0.31
Specificity	0.73	0.81	0.71	0.83	0.77

It can be observed in the testing dataset that the precision and sensitivity results are low 0.31. In contrast, the accuracy reached is 0.66 and a specificity of 0.77. The low value of sensitivity indicates a low percentage of persons with skin cancer who are correctly identified by the proposed method. In contrast, the high value of specificity indicates a high percentage of persons without the disease who are correctly excluded by our algorithm. "Clinically, these concepts are important for confirming or excluding disease during screening. Ideally, a test should provide high sensitivity and specificity" (99).

When comparing the accuracy of the test set with the accuracy of the validation set, it observed that it is lower, 0.66 and 0.74, respectively. It most likely, when improving the algorithm taking into account the behavior of the validation data, we are involuntarily influencing the model. So that in favor of the images of the validation set is adapted. For this reason, it is essential to include the test set, which allows a more objective evaluation of the model.

Finally, the table 7 shows the results obtained by the proposed method and the results obtained by other works that also use convolutional neural networks. As we can see, our results do not exceed them. However, this may be because we need a more substantial database since, as we can see in the table 7, the results vary according to the amount of the dataset and how many classes will be classified. For example, E. Nasr-Esfahani et al. (40) used a dataset of 6120 images and got an accuracy of 0.81, a sensitivity of 0.81, and a specificity of 0.80 for a problem of binary classification between melanoma or benign. On the other hand, Mendes et al. (98) used a bigger dataset of 111069 images. However, it obtained an accuracy of 0.78 because the algorithm proposed by the authors tried to qualify 11 skin lesions. Then, considering that the proposed method faces a multiclass classification problem of four classes and that the dataset employed is smaller than that used by E. Nasr-Esfahani et al. for binary classification, the use of a more extensive database could generate better results.

Table 7. Quantitative comparison with other works. Source: Prepared by authors.

Authors	Total dataset	Classes	Accuracy	Sensitivity	Specificity
Mendes et al (98)	111,069	11	0.78	-	-
E. Nasr-Esfahani et al (37)	6,120	2	0.81	0.81	0.80
Proposed	1,000	4	0.66	0.31	0.77

4.6 Graphic user interface (GUI)

A graphical interface was programmed in Python using Tkinter package (96) to graphically show the operation performed by the convolutional neural network to the detection of skin cancer. Also, information about sun protection has included. The process of the GUI is simple. First, the main window (Fig 38.A) contains two options to check your skin and tips. When selecting the check your skin option, a new window appears showing three buttons- Open Image, image processing, and return (Fig 38.B). By pressing the Open Image button, an image is loaded and shows in the window. Once the image is loaded, if the processing image button pressed (Fig 38. C), the software automatically returns the prediction made by the CNN and the preprocessed image (Fig 38. D). User can press the image button again to load a different image and make a new one prediction. Moreover, when selecting the tips option, a new window appears showing some informative tips related to skin cancer protection (Fig 38. E). Back buttons allow us to return to the main window.

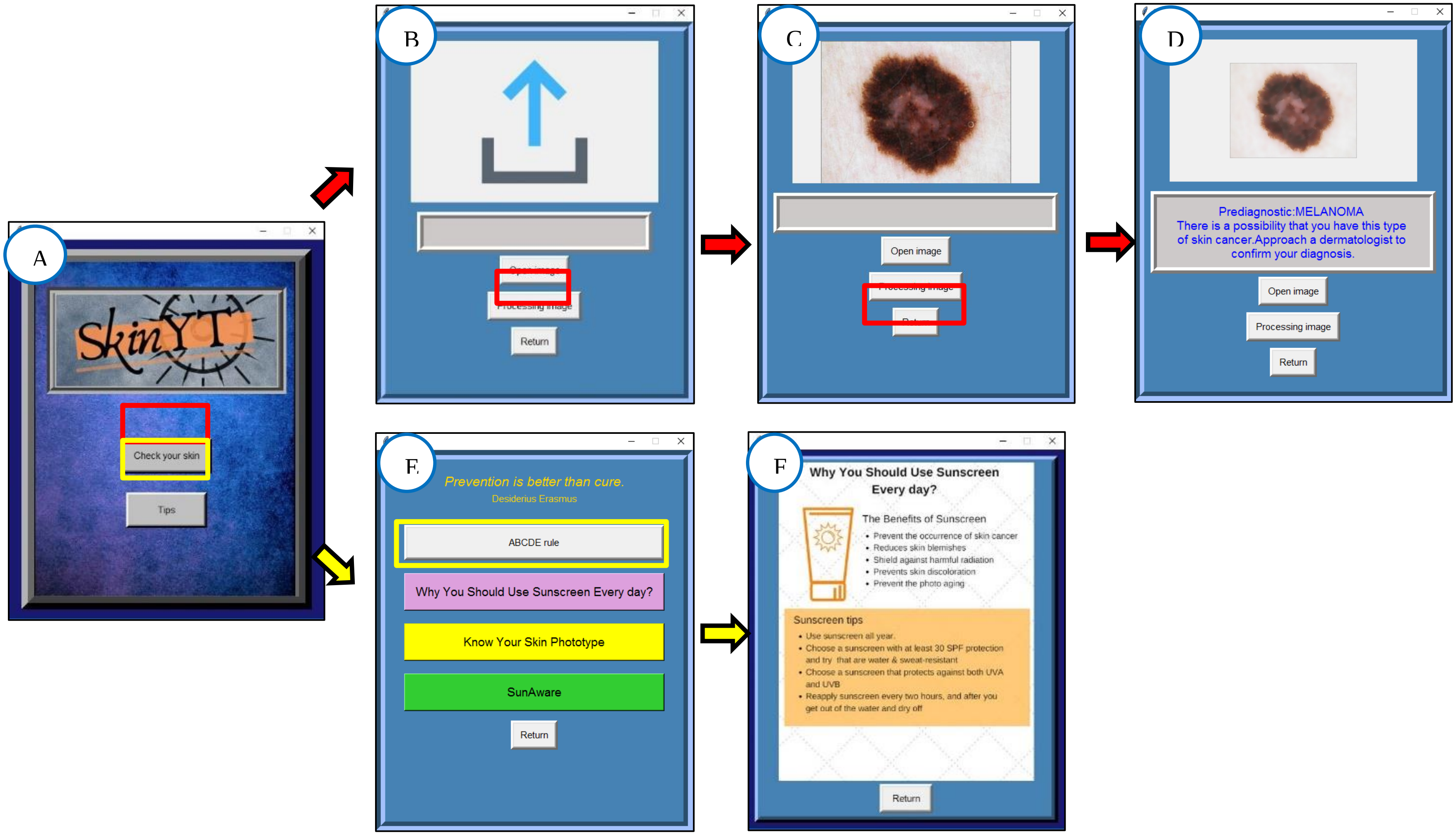

Figure 38. Proposed Graphic user interface (GUI). Source: Prepared by authors.

5 Conclusions and future work

5.1 Conclusions

Surveys conducted in the city of Otavalo, specifically in the Plaza de Los Ponchos market, show us that most people know about the damage caused by solar radiation to the skin. Also, they keep in mind that the accumulation of solar radiation can cause skin cancer in adulthood. However, they do not take good care of UV radiation even though they spend more time under the sun due their work.

In Ecuador, the radiation arrives almost perpendicularly on the earth's surface because of its localization in the equinoctial line. When comparing the aerosol optical depths at 550nm (AOD550nm) in the two cities Otavalo and Cañaveral, we obtained that Cañaveral has a higher value (0.065±0.025) than Otavalo. Besides, Cañaveral also presented higher total ozone columns (256±10) Dobson Units than Otavalo. These results contribute to the passage of a large amount of UV radiation in Otavalo. On the other hand, in the modeling of UV radiation, we obtained that Otavalo city has higher irradiance in all ranges, which is logical because it has a higher altitude. Then, the annual mean irradiances in Otavalo exceed with a value of 37.5 Wm-2 to Cañaveral. In addition to this, the lack of education on sun protection increases the risk of developing skin cancer in Otavalo.

A dataset of skin cancer images presented, a preprocessing algorithm, and a convolutional neural network proposed to its classification into four different classes - basal cell carcinoma, benign, melanoma, and squamous cell carcinoma. Due to the quantity and quality of the images of the dataset proposed, the accuracy, sensitivity, and specificity results obtained were 0.66, 0.31, and 0.77, respectively. These results do not exceed the results obtained by other skin cancer detection algorithms. So, it would be to get more skin lesions images that help improve the convolutional neural network to better classification performance.

5.2 Future work

Part of the future work for an Ecuadorian application to skin cancer detection using Convolutional Neural Networks CNN is to increase the images dataset and improve the image quality. For example, to seek collaboration with hospitals and clinics to obtain a large number of pictures of each type of skin cancer, which included in the application. Also, investigate the best conditions to capture a skin lesion image using a digital camera to create a protocol so that all the photos in the database will be of a very similar quality, which would facilitate the preprocessing stage of the image. Then, training the net again with a longer duration to improve its accuracy, sensitivity, and specificity. The use of different image distributions in the training, validation, and test groups could be a way to achieve it. The final step would optimize the algorithm so that it can work on a mobile phone and include a large amount of relevant information related to skin cancer, sun protection, UV radiation, and other topics similar to these. To the aim that a large number of people can use it and they know about skin cancer and protect themselves against this disease.

REFERENCES

1. Skin Cancer Foundation. Skin Cancer Facts & Statistics [Internet]. ©2019 The Skin Cancer Foundation A 501(c)(3). 2019. Available from: https://www.skincancer.org/skin-cancer-information/skin-cancer-facts/

2. American Cancer Society. Key Statistics for Melanoma Skin Cancer [Internet]. 2019. Available from: https://www.cancer.org/cancer/melanoma-skin-cancer/about/key-statistics.html

3. World Cancer Research Fund International. Skin cancer statistics [Internet]. 2018 [cited 2019 Dec 4]. Available from: https://www.wcrf.org/dietandcancer/cancer-trends/skin-cancer-statistics

4. American Cancer Society. Risk Factors for Melanoma Skin Cancer [Internet]. © 2019 American Cancer Society, Inc. 2019. Available from: https://www.cancer.org/cancer/melanoma-skin-cancer/causes-risks-prevention/risk-factors.html

5. Jara C, Mercedes J. Efectos de la radiación solar en la piel. 2015;4:5–6.

6. Gonzáles M, Vernhes M, Sánchez A. La radiación ultravioleta. Su efecto dañino y consecuencias para la salud humana. Theoria [Internet]. 2009;18(2):69–80. Available from: https://www.ubiobio.cl/miweb/webfile/media/194/v/v18-2/06.pdf

7. Huaca P JM, Salum GM, Placentini RD. Solar erythemal irradiance in Ibarra, Ecuador (high altitude equatorial city). Ground and satellite measurements and model calculations. Bionatura [Internet]. 2018;3(1). Available from: http://revistabionatura.com/files/2018.03.01.3.pdf

8. Pedro Lobos B, Andrea Lobos S. Cáncer de piel no-melanoma. Rev Médica Clínica Las Condes [Internet]. 2011;22(6):737–48. Available from: http://dx.doi.org/10.1016/S0716-8640(11)70486-2

9. Rigel DS. Cutaneous ultraviolet exposure and its relationship to the development

of skin cancer. J Am Acad Dermatol. 2008;58(5 SUPPL. 2).

10. National Institute of Health Consensos Development Conference Statements. Sunlight, Ultraviolet Radiation, and the Skin. [Internet]. Vol. 7(8). 1989. p. 1–29. Available from: https://consensus.nih.gov/1989/1989SunUVSkin074html.htm

11. American Cancer Society. Key Statistics for Basal and Squamous Cell Skin Cancers [Internet]. 2019 [cited 2020 Feb 25]. Available from: https://www.cancer.org/cancer/basal-and-squamous-cell-skin-cancer/about/key-statistics.html

12. Pam American Health Organization, World Health Organization. HEALTH INDICATORS: Conceptual and operational considerations (Section 2) [Internet]. [cited 2020 Feb 5]. p. 3. Available from: https://www.paho.org/hq/index.php?option=com_content&view=article&id=14402:health-indicators-conceptual-and-operational-considerations-section-2&Itemid=0&limitstart=2&lang=en

13. Guayaquil S. Gráfico 2. Distribución por diagnóstico por sexo. 2019;(Gráfico 2):12–5. Available from: http://www.estadisticas.med.ec/Publicaciones/1 Reporte Incidencia Solca 2014-2018- 0-14a.pdf

14. Mora Moraima, Olivares Alvis, MelaTania GM. The sun: enemy of our skin? MEDISAN [Internet]. 2010;14(6):825. Available from: http://scielo.sld.cu/pdf/san/v14n6/san14610.pdf

15. Castañeda P, Eljure J. Cancer de piel un problema actual. Artic Revis [Internet]. 2016;59(2):6–14. Available from: https://www.medigraphic.com/pdfs/facmed/un-2016/un162b.pdf

16. Mayo Clinic. Skin Cancer [Internet]. 2019. Available from: https://www.mayoclinic.org/diseases-conditions/skin-cancer/symptoms-causes/syc-20377605

17. Women's Health Matters. Nonmelanoma Skin Cancer [Internet]. Women's

College Hospital. [cited 2020 Feb 9]. Available from: https://www.womenshealthmatters.ca/health-centres/skin-cancer/nonmelanoma-skin-cancer/

18. Rigel DS. Cutaneous ultraviolet exposure and its relationship to the development of skin cancer. J Am Acad Dermatol [Internet]. 2008 May 1 [cited 2019 Aug 21];58(5):S129–32. Available from: https://www.sciencedirect.com/science/article/abs/pii/S0190962207024139?via%3Dihub

19. Matriz S. Compendio de Indicadores epidemiológicos y prestación de. 2019;

20. MacKie RM. Long-term health risk to the skin of ultraviolet radiation. Prog Biophys Mol Biol. 2006;92(1):92–6.

21. Badash I, Shauly O, Lui CG, Gould DJ, Patel KM. Nonmelanoma Facial Skin Cancer: A Review of Diagnostic Strategies, Surgical Treatment, and Reconstructive Techniques. Clin Med Insights Ear, Nose Throat [Internet]. 2019;12:117955061986527. Available from: http://journals.sagepub.com/doi/10.1177/1179550619865278

22. Veness MJ, Delishaj D, Barnes EA, Bezugly A, Rembielak A, Library C. Current Role of Radiotherapy in Non-melanoma Skin Cancer Statement of Search Strategies Used and Sources of Information Radiotherapy in Non-melanoma Skin Cancer. Clin Oncol [Internet]. 2019;(xxxx). Available from: https://doi.org/10.1016/j.clon.2019.08.004

23. Estela N, Gonz H, Yasm A, Flores A. El melanoma en México. Rev Espec Médico-Quirúrgicas. 2010;15(3):161–4.

24. American Cancer Society. What Is Melanoma Skin Cancer? [Internet]. 2019 [cited 2019 Dec 19]. Available from: https://www.cancer.org/cancer/melanoma-skin-cancer/about/what-is-melanoma.html

25. Centro de Atención Dermatológica Integral Cadermint S.A. Lentigos – Nevos –

Cáncer de Piel [Internet]. 2019 [cited 2019 Dec 3]. Available from: http://cadermint.ec/web/seccion/detalle?data=aWRTZWNjaW9uPTU5

26. Shitara D, Tell-Martí G, Badenas C, Enokihara MMSS, Alõs L, Larque AB, et al. Mutational status of naevus-associated melanomas. Br J Dermatol. 2015;173(3):671–80.

27. American Cancer Society. Signs and Symptoms of Basal and Squamous Cell Skin Cancers [Internet]. 2019 [cited 2020 Feb 25]. Available from: https://www.cancer.org/cancer/basal-and-squamous-cell-skin-cancer/detection-diagnosis-staging/signs-and-symptoms.html

28. Cavalcanti PG, Scharcanski J, Baranoski GVG. A two-stage approach for discriminating melanocytic skin lesions using standard cameras. Expert Syst Appl [Internet]. 2013;40(10):4054–64. Available from: http://dx.doi.org/10.1016/j.eswa.2013.01.002

29. Alcón JF, Kate W, Heinrich A, Uzunbajakava N, Krekels G, Siem D, et al. for Inspection of Pigmented Skin Lesions and Melanoma Diagnosis. 2009;3(1):14–25.

30. Sordo C, Gutiérrez C. Cáncer de piel y radiación solar: experiencia peruana en la prevención y detección temprana del cáncer de piel y melanoma. Rev Peru Med Exp Salud Publica. 2013;30(1):113–7.

31. Pflugfelder A, Kochs C, Blum A, Capellaro M, Czeschik C, Dettenborn T, et al. Malignes melanom S3-leitlinie “Diagnostik, therapie und nachsorge des melanoms.” JDDG - J Ger Soc Dermatology. 2013;11(SUPPL. 6):1–126.

32. bertel technology. COMPUTER VISION SYSTEMS [Internet]. 1996 [cited 2020 Feb 26]. Available from: https://www.isdngroup.com/division-de-automatizacion-industrial/sistemas-de-vision-artificial/

33. Li Y, Esteva A, Kuprel B, Novoa R, Ko J, Thrun S. Skin cancer detection and tracking using data synthesis and deep learning. AAAI Work - Tech Rep. 2017;WS-17-01-:551–4.

34. Kalwa U, Legner C, Kong T, Pandey S. Skin cancer diagnostics with an all-inclusive smartphone application. Symmetry (Basel). 2019;11(6).

35. Nazneen N Sultana NBP. Recent Deep Learning Methods for Melanoma Detection: A Review. 2018;(April):749–56. Available from: http://dx.doi.org/10.1007/978-981-13-0023-3_8

36. University of Alcalá. Advantages and Disadvantages of the Use of Artificial Intelligent [Internet]. 2019 [cited 2019 Dec 4]. Available from: https://master-deeplearning.com/ventajas-desventajas-inteligencia-artificial/

37. Esteva A, Kuprel B, Novoa RA, Ko J, Swetter SM, Blau HM, et al. Dermatologist-level classification of skin cancer with deep neural networks. Nature [Internet]. 2017;542(7639):115–8. Available from: http://dx.doi.org/10.1038/nature21056

38. Rosebrock A. OpenCV Gamma Correction [Internet]. pyimagesearch. 2015 [cited 2019 Oct 21]. Available from: https://www.pyimagesearch.com/2015/10/05/opencv-gamma-correction/

39. Celebi ME, Kingravi HA, Iyatomi H, Aslandogan YA, Stoecker W V., Moss RH, et al. Border detection in dermoscopy images using statistical region merging. Ski Res Technol. 2008;14(3):347–53.

40. Nasr-Esfahani E, Samavi S, Karimi N, Soroushmehr SMR, Jafari MH, Ward K, et al. Melanoma detection by analysis of clinical images using convolutional neural network. Proc Annu Int Conf IEEE Eng Med Biol Soc EMBS. 2016;2016-Octob:1373–6.

41. Arbara B, Ilchrest a G, Ller PEHD, Lan A, Eller CG, Ina M, et al. Mechanisms of Disease T He P Athogenesis of M Elanoma I Nduced By U Ltraviolet R Adiation. N Engl J Med. 1999;340(17):1341–8.

42. World Health Organization, World Meteorological Organization, United Nations Environment Programme, International Commision on Non-Ionizing Radiation Protection. GLOBAL SOLAR UV INDEX A Practical Guide. 2002.

43. Sailor DJ, Resh K, Segura D. Field measurement of albedo for limited extent test surfaces. Sol Energy. 2006;80(5):589–99.

44. Cao J, Chen E, Cheng J. Broadband Albedo. In: Advanced Remote Sensing. Elsevier Inc.; 2012. p. 175–233.

45. Przyborski P. global albedo [Internet]. visible earth. 2002 [cited 2020 Jan 28]. Available from: https://visibleearth.nasa.gov/images/60636/global-albedo

46. Stackhouse P. NASA Prediction of Worldwide Energy Resource (POWER) [Internet]. NASA. 2005 [cited 2020 Jan 28]. Available from: https://power.larc.nasa.gov/data-access-viewer/

47. R. R. Dickerson, S. Kondragunta GS, K. L. Civerolo, B. G. Doddridge BNH. The Impact of Aerosols on Solar Ultraviolet radiation and Photochemical Smog. Science (80-). 1997;278:827–30.

48. Laura A, Peña P, Baró R, Jimenez Guerrero P. Estudio del efecto directo de los aerosoles atmosféricos sobre Europa. 2014;8–13.

49. Iqbal M. A CLOUDLESS-SKY ATMOSPHERE. In: An Introduction to Solar Radiation. 1983. p. 85–105.

50. Gonzalez Navarrete JC, Salamanca J. Aplicación del método dobson a la estimación del ozono total utilizando un radiómetro ultravioleta. Rev Mex Fis. 2012;58(6):497–503.

51. Iqbal M. Solar Spectral Radiation Under Cloudless Skies. In: Introduction to Solar Radiation. 1983. p. 124–6.

52. Coddington O, University of Colorado - LASP. Solar Spectral Irradiance [Internet]. National Oceanic and Atmospheric Administration. [cited 2020 Jan 28]. Available from: https://www.ncdc.noaa.gov/cdr/atmospheric/solar-spectral-irradiance

53. National Aeronautics and Space Administration. Solar Irradiance [Internet].

NASA. 2017. Available from: https://www.nasa.gov/mission_pages/sdo/science/solar-irradiance.html

54. Raponi M, Wolfram E, Pallotta JV, Piacentini R. Medición y modelización de la irradiancia espectral solar UV incidente sobre Buenos Aires, Argentina. Determinación de irradiancia eritémica. An AFA. 2004;16(January):283–6.

55. Emery K, Myerds D. Reference Solar Spectral Irradiance: Air Mass 1.5 [Internet]. Center, RERD, Ed. 2009. Available from: https://rredc.nrel.gov/solar//spectra/am1.5/

56. Gueymard C. SMARTS2 , A Simple Model of the Atmospheric Radiative Transfer of Sunshine : Algorithms and performance assessment [Internet]. Cocoa, Florida: Florida Solar Energy Center; 1995. 270–295 p. Available from: http://www.fsec.ucf.edu/en/publications/pdf/FSEC-PF-270-95.pdf?fbclid=IwAR2b9U9ydN0T_o931pscijh2MLnC7GvqkbEew68SVrtiaMjGXij31jX_8yM

57. Navy Environmental Health Center. Ultraviolet Radiation Guide. 2510 Walmer Ave Norfolk, Virginia, 23513-2617. 1992;(April).

58. Parrish JA, Jaenicke K, Anderson RR. Erythema and Melanogénesis Action Spectra of Normal Human Skin. Photochem Photobiol. 1982;36(2):187–91.

59. Latimer JA, Lloyd J, Diffey B, Matts P, Birch-machin MA, Latimer JA, et al. Determination of the Action Spectrum of UVR-Induced Mitochondrial DNA Damage in Human Skin Cells. J Invest Dermatol [Internet]. 2015;135:2512–8. Available from: http://dx.doi.org/10.1038/jid.2015.194

60. Acker J, Soebiyanto R, Kiang R, Kempler S. Use of the NASA giovanni data system for geospatial public health research: Example of weather-influenza connection. ISPRS Int J Geo-Information. 2014;3(4):1372–86.

61. National Aeronautics and Space Administration. Atmospheric Aerosols: What Are They, and Why Are They So Important? [Internet]. 2017 [cited 2020 Jan 14].

Available from:
https://www.nasa.gov/centers/langley/news/factsheets/Aerosols.html

62. Sánchez F. Consideraciones sobre la capa con el cáncer de piel. Rev Médica Chile [Internet]. 2006;(134):1185–90. Available from: https://scielo.conicyt.cl/pdf/rmc/v134n9/art15.pdf

63. Gueymard C. SMARTS code, version 2.9.5 User's Manual [Internet]. Solar Consulting Services; 2005. p. 2–49. Available from: file:///C:/Users/Juan/Desktop/tesis/factores que involucran en la radiacion solar/SMARTS295_Users_Manual_Mac.pdf

64. American Cancer Society. Ultraviolet (UV) Radiation [Internet]. 2020 [cited 2020 Jan 28]. Available from: https://www.cancer.org/cancer/cancer-causes/radiation-exposure/uv-radiation.html

65. Pareja E. ACCION DE LOS AGENTES FISICOS SOBRE LAS BACTERIAS (II) [Internet]. Curso de Microbiología General de Enrique Iáñez. 1998 [cited 2020 Feb 26]. Available from: http://www.biologia.edu.ar/microgeneral/micro-ianez/18_micro.htm

66. Bastidas RHA. Reflexiones sobre la aplicación de la transformada de fourier al procesamiento digital de imágenes. [Internet]. FUNDACIÓN UNIVERSITARIA KONRAD LORENZ; 2010. Available from: http://www.konradlorenz.edu.co/images/investigaciones/matematicas/procesamiento_imagenes_fourier.pdf

67. Ennehar B, Brahim O, Hicham T. An Appropriate Color Space to Improve Human Skin Detection. INFOCOMP J Comput Sci. 2010;9(4):1–10.

68. Bull D. Digital Picture Formats and Representations. In: Elsevier Ltd, editor. Communicating Pictures [Internet]. 2014. p. 99–132. Available from: https://www.sciencedirect.com/science/article/pii/B9780124059061000040

69. Olabe XB. REDES NEURONALES ARTIFICIALES [Internet]. Publicaciones de

la Escuela de Ingenieros; 1998. Available from: http://cvb.ehu.es/open_course_ware/castellano/tecnicas/redes_neuro/contenidos/pdf/libro-del-curso.pdf

70. Moreno A, Armengol E, Bejar E, Belanche L, Cortez U, Gavalda R, et al. Aprendizaje automático [Internet]. 1994. Available from: https://upcommons.upc.edu/handle/2099.3/36157

71. Fogel AL, Kvedar JC. Artificial intelligence powers digital medicine. npj Digit Med. 2018;1(1):3–6.

72. Miller DD, Brown EW. Artificial Intelligence in Medical Practice: The Question to the Answer? Am J Med [Internet]. 2018;131(2):129–33. Available from: https://doi.org/10.1016/j.amjmed.2017.10.035

73. Matteo Testi & Francesco Pugliese. Una breve mirada al Aprendizaje Profundo y el Aprendizaje Automático [Internet]. DeepLarningItalia. 2017 [cited 2020 Jan 6]. Available from: https://www.deeplearningitalia.com/una-breve-mirada-al-aprendizaje-profundo-y-el-aprendizaje-automatico/

74. Arel I, Rose DC, Karnowski TP. Deep Machine Learning — A New Frontier in Artificial Intelligence Research. 2010;(November):13–8.

75. Lopez CP. Redes Neuronales. In: CreateSpace Independent Publishing Platform, editor. Redes Neuronales A Traves De Ejemplos Aplicaciones Con Matlab [Internet]. 2017. p. 158. Available from: https://books.google.com.ec/books?id=fl3HswEACAAJ&dq=red+neuronal&hl=es&sa=X&ved=0ahUKEwiVmvS_rYvmAhUi1lkKHY12CvYQ6AEINjAC

76. Stanford University CS231n course. CS231n Convolutional Neural Networks for Visual Recognition [Internet]. p. Module 1: Neural Networks. Available from: http://cs231n.github.io/

77. A. Requena, R. Quintanilla, J.M. Bolarín, A. Vázquez, A. Bastida JZ y LMT. Equivalencia entre redes artificiales y biológicas. In: Nuevas Tecnologías y

Contaminación de Atmósferas, para PYMEs [Internet]. Universidad de Murcia. Spain; [cited 2020 Jan 7]. p. 3. Available from: https://www.um.es/LEQ/Atmosferas/Ch-VI-3/F63s4p3.htm

78. Nielsen M. Neural Networks and Deep Learning. Artif Intell. 2018;167–85.

79. O'Shea K, Nash R. An Introduction to Convolutional Neural Networks. 2015;(December). Available from: http://arxiv.org/abs/1511.08458

80. Sharma N, Jain V, Mishra A. An Analysis of Convolutional Neural Networks for Image Classification. Procedia Comput Sci [Internet]. 2018;132(Iccids):377–84. Available from: https://doi.org/10.1016/j.procs.2018.05.198

81. National Aeronautics and Space Administration. Convolutional Neural Networks Tutorial in TensorFlow [Internet]. 2017 [cited 2020 Jan 6]. Available from: https://adventuresinmachinelearning.com/convolutional-neural-networks-tutorial-tensorflow/

82. Costa V. Understanding the Structure of a CNN [Internet]. 2019 [cited 2020 Jan 6]. Available from: https://mc.ai/understanding-the-structure-of-a-cnn/

83. Chen Zimo H. Deeplearning - Overview of Convolution Neural Network [Internet]. 2018 [cited 2020 Jan 10]. Available from: https://www.zybuluo.com/hongchenzimo/note/1086311

84. Moedvintsev A, Rahman A. Introduction to OpenCV-Python Tutorials [Internet]. OpenCV-Python. 2013 [cited 2020 Mar 3]. Available from: https://opencv-python-tutroals.readthedocs.io/en/latest/py_tutorials/py_setup/py_intro/py_intro.html.

85. Keras Documentation. Keras: The Python Deep Learning library [Internet]. GitHub. Available from: https://keras.io/

86. Dertat A. Applied Deep Learning - Part 4: Convolutional Neural Networks [Internet]. Towards data science. 2017 [cited 2020 Mar 4]. Available from: https://towardsdatascience.com/applied-deep-learning-part-4-convolutional-neural-

networks-584bc134c1e2

87. Rosebrock A. OpenCV Gamma Correction [Internet]. 2015 [cited 2020 Jan 8]. Available from: https://www.pyimagesearch.com/2015/10/05/opencv-gamma-correction/

88. GitHub. puigalex/AMP-Tech [Internet]. 2020 [cited 2020 Jan 15]. Available from: https://github.com/puigalex/AMP-Tech/tree/master/CNN desde cero

89. GitHub. Keras Documentation [Internet]. 2020 [cited 2020 Jan 15]. Available from: https://keras.io/layers/core/

90. Mikulski B. Understanding the softmax activation function [Internet]. 2016. Available from: https://www.mikulskibartosz.name/understanding-the-softmax-activation-function/

91. Verma A. Keras ImageDataGenerator methods: An easy guide [Internet]. Keras. 2018 [cited 2020 Feb 26]. Available from: https://medium.com/datadriveninvestor/keras-imagedatagenerator-methods-an-easy-guide-550ecd3c0a92

92. Baranwal A, Khatri A, Baranwal T. Splitting data into train, validation, and test data. In: What’s New in TensorFlow 20 [Internet]. Packt Publ. 2019. p. 54. Available from: https://books.google.com.ec/books?id=e--oDwAAQBAJ&pg=PA54&lpg=PA54&dq=80+10+10+split+machine+learning&source=bl&ots=CqlQSIF1Gb&sig=ACfU3U3uqqY_p3nPHxyVy702gGHu5yoeBw&hl=es&sa=X&ved=2ahUKEwiq5dv6xv7nAhUOXK0KHeOCCVQQ6AEwD3oECAkQAQ#v=onepage&q=80 10 10 split machine learning&f=false

93. Padmanabhan A, Dubey PK. Confusion Matrix [Internet]. 2019 [cited 2020 Jan 15]. Available from: https://devopedia.org/confusion-matrix

94. Sharma P. Decoding the Confusion Matrix [Internet]. Towards data science. 2019 [cited 2020 Jan 15]. Available from: https://towardsdatascience.com/decoding-the-confusion-matrix-bb4801decbb

95. Contreras OE. Desarrollo de una red neuronal convolucional para el procesamiento de imágenes placentarias [Internet]. 2018. Available from: https://pdfs.semanticscholar.org/f379/d8a0922b090b6bc631aa4da3ac17a27c983d.pdf

96. Python Software Foundation. tkinter — Python interface to Tcl/Tk [Internet]. 2001 [cited 2020 Feb 26]. Available from: https://docs.python.org/3/library/tkinter.html

97. OpenCV. Image Filtering [Internet]. 2011 [cited 2020 Jan 17]. Available from: https://docs.opencv.org/2.4/modules/imgproc/doc/filtering.html#image-filtering

98. Mendes DB, da Silva NC. Skin Lesions Classification Using Convolutional Neural Networks in Clinical Images. 2018; Available from: http://arxiv.org/abs/1812.02316

99. Boyce D. Evaluation of Medical Laboratory Tests [Internet]. 3rd ed. Orthopaedic Physical Therapy Secrets: Third Edition. Elsevier Inc.; 2017. 125–134 p. Available from: http://dx.doi.org/10.1016/B978-0-323-28683-1.00017-5

ANNEXES

Annex 1. Survey

UNIVERSIDAD DE INVESTIGACIÓN DE TECNOLOGÍA EXPERIMENTAL YACHAY

ESCUELA DE CIENCIAS BIOLÓGICAS E INGENIERÍA

CARRERA: BIOMEDICINA

Objetivo: Determinar el nivel de conocimiento acerca de cáncer de piel y su prevención en las personas de Otavalo. Por favor sírvase contestar las siguientes preguntas.

DATOS INFORMATIVOS

Género: Femenino ____ Masculino ____

Edad: _____

Nivel académico: Primaria ____ Secundaria ____ Superior ____ Ninguno ____

1. Lugar donde vive:

   Zona rural ____ Zona urbana ____

2. Ocupación: ___________________

3. ¿Ha escuchado hablar sobre cáncer de piel?

   Si ____ No ____

4. ¿Sabía que la acumulación de radiación solar es uno de los factores para desarrollar cáncer de piel en la edad adulta?

   Si ____ No ____

5. ¿Se protege usted del sol?

   Si ____ No ____

6. ¿Cómo se protege de la radiación solar?

Protector solar ____

Sombrero ____

Camisa manga larga ____

Gafas ____

Sombrilla ____

Se pone a la sombra ____

Ninguna de las anteriores ____

7. ¿Ha asistido a una consulta dermatológica?

   Si ____ No ____

   Si su respuesta es afirmativa. Escriba el motivo de la consulta:

   ____

8. ¿Presta atención a sus lunares (cambio de forma, tamaño, textura y color)?

   Si ____ No ____

9. ¿ Usaría una aplicación que le ayude a examinar los lunares mediante la toma de imágenes para prevenir el riesgo de cáncer de piel?

   Si ____ No ____

10. Señale cuál de estos tipos de piel cree que es la suya:

    Me quemo muy fácilmente con el sol ____

    A veces me quemo con el sol ____

    Casi nunca me quemo con el sol ____

    Nunca me quemo con el sol ____

11. Evita el sol entre las 11 a 14 horas?

    Siempre ____

    Casi Siempre ____

    Casi nunca ____

    Nunca ____

12. ¿ Tiene hijos?

    Si ____ No ____

    Si la respuesta anterior es afirmativa. Conteste las siguientes preguntas:

13. ¿Cree que es necesario que los niños se protejan del sol?

    Si ____ No ____

14. ¿Cuál de estos métodos de protección solar utiliza su hijo/a?

Protector solar ____

Sombrero ____

Camisa manga larga ____

Gafas ____

Sombrilla ____

Se pone a la sombra ____

Ninguna de las anteriores ____

15. Alguna vez su hijo/a cuando se expuso al sol presentó:

    Se quedó rojo ____

    Ardor ____

    Ampollas ____

    Peladura ____

!GRACIAS POR SU COLABORACIÓN !

Annex 2. Cadermint S.A brochures

"Prevención del cancer de piel" brochure.

"Observa tu piel" brochure.


Otras señales
Lunar que sangra, pica
Lunar que crece rápido
Lunar con escama o costra
Llaga que no se cura
Recomendaciones
Evite el Sol entre las 11 -14 horas
Evite lámparas o cabinas bronceadoras
Use sombrero de ala ancha, gorra, gafas, ropa de trama compacta y tonos oscuros, guantes de manejo si conduce
No exponer mucho a los niños antes de los 2 años
Use protector solar de amplio espectro UVB - UVA en areas expuestas, orejas, cuello y pies
El agua, arena, nieve reflejan RUV, reforzar la protección
Mismas recomendaciones en dias nublados
Beber líquidos
Use cremas hidratantes después de estar en el Sol
Si alguna "peca" cambia de color o crece, consulte al dermatólogo
Algunos medicamentos reaccionan con el Sol. . . consulte!!
Difunda esta información a sus familiares
Umbrella
Intelligent
Protector solar SPF 100, de amplio espectro UVB, protección UV HEV, IR-A.
PARA TODO TIPO DE PIEL
medihealth
Cadermint s.a.
Centro de Atención Dermatológica Integral S.A.
QUITO-ECUADOR
Observa tu piel
Campaña de prevención del cáncer de piel en el Ecuador
Mientras más temprano se detecte el cáncer de la piel más éxito en el tratamiento
www.cadermint.ec

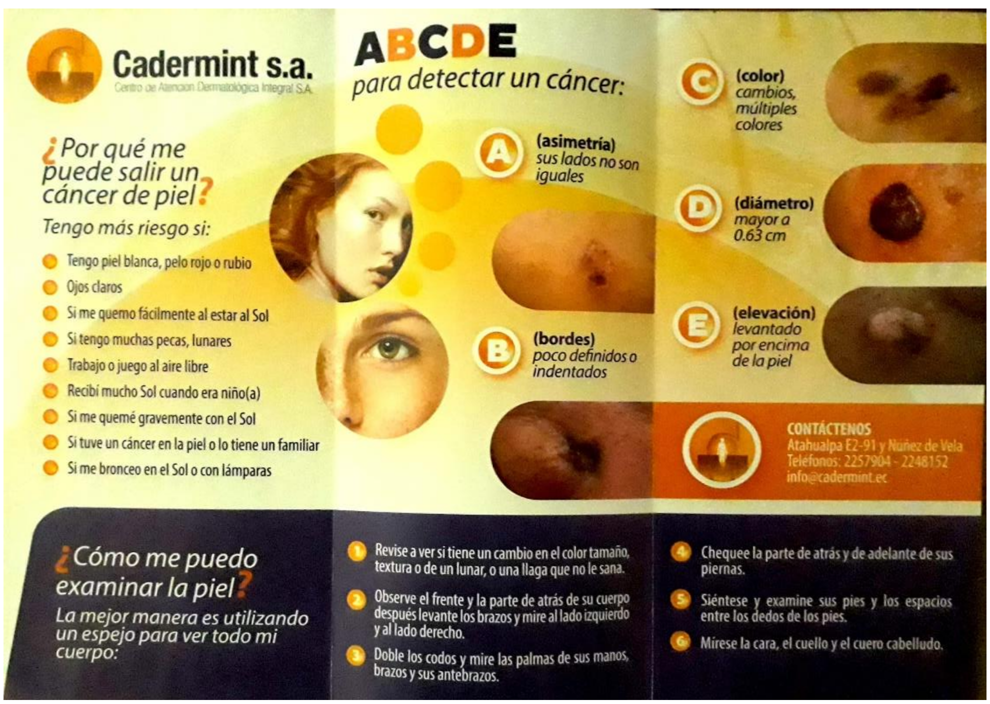
Cadermint s.a.
Centro de Atencion Dermatológica Integral S.A.
¿Por qué me puede salir un cáncer de piel?
Tengo más riesgo si:
Tengo piel blanca, pelo rojo o rubio
Ojos claros
Si me quemo fácilmente al estar al Sol
Si tengo muchas pecas, lunares
Trabajo o juego al aire libre
Recibí mucho Sol cuando era niño(a)
Si me quemé gravemente con el Sol
Si tuve un cáncer en la piel o lo tiene un familiar
Si me bronceo en el Sol o con lámparas
ABCDE
para detectar un cáncer:
A (asimetría) sus lados no son iguales
B (bordes) poco definidos o indentados
C (color) cambios, múltiples colores
D (diámetro) mayor a 0.63 cm
E (elevación) levantado por encima de la piel
CONTÁCTENOS
Atahualpa E2-91 y Nuñez de Vela
Teléfonos: 2257904 - 2248152
info@cadermint.ec
¿Cómo me puedo examinar la piel?
La mejor manera es utilizando un espejo para ver todo mi cuerpo:
1 Revise a ver si tiene un cambio en el color tamaño, textura o de un lunar, o una llaga que no le sana.
2 Observe el frente y la parte de atrás de su cuerpo después levante los brazos y mire al lado izquierdo y al lado derecho.
3 Doble los codos y mire las palmas de sus manos, brazos y sus antebrazos.
4 Chequee la parte de atrás y de adelante de sus piernas.
5 Siéntese y examine sus pies y los espacios entre los dedos de los pies.
6 Mírese la cara, el cuello y el cuero cabelludo.

Annex 3. Results of survey

Survey of 50 people from Otavalo, handicraft market Plaza de los Ponchos.

Age	Women	Women percentage	Men	Men percentage	Total
12 to 17	5	10%	1	2%	6
18 to 29	11	22%	6	12%	17
30 to 59	14	28%	11	22%	25
Above 60	1	2%	1	2%	2
Total	31	62%	19	38%	50

Table and figure show the results of the number of respondents divided by gender.

Education Level	Frequency	Percentage
Elementary	14	28%
High school	21	42%
University	14	28%
None	1	2%
Total	15	100%

Table and figure show the results of the level of educational preparation, dividing into Elementary, Hign school, University and none.

Where do you live?

Zone	Frequency	Percentage
Rural	18	36%
Urban	32	64%
Total	50	100%

Result of the place where respondents live: 36% rural zone, and 64% urban zone.

What is your profession?

Profession	Frequency	Percentage
Craftsman-Merchant	30	60%
Craftsman-student	14	28%
Housemaid	3	6%
Public employee	1	2%
Teacher	1	2%
Journalist	1	2%
Total	50	100%

The results show that the majority of respondents are purely craftsman-merchant.

Do you heard about skin cancer?

Options	Frequency	Percentage
Yes	44	88%
No	6	12%
Total	50	100%

Table and figure demonstrate the result that 88% know about skin cancer.

Did you know that the accumulation of solar radiation is one of the factors to develop skin cancer in adulthood?

Options	Frequency	Percentage
Yes	34	68%
No	16	32%

Total	50	100%

68% of respondents know that the accumulation of solar radiation is the main factor in developing skin cancer.

Do you protect yourself from the sun?

Options	Frequency	Percentage
Yes	45	90%
No	5	10%
Total	50	100%

This table and figure show that 90% of respondents protect from the sun

How do you protect yourself from solar radiation?

Protection	Frequency	Percentage
Sunscreen	34	68%
Hat	38	76%
Long sleeve jersey	33	66%
Sunglasses	8	16%
Umbrella	1	2%
Shadow	38	76%
None	1	2%

Ways in which respondents protect themselves from solar radiation.

Have you attended a dermatological consultation?

Options	Frequency	Percentage

Yes	8	16%
No	42	84%
Total	50	100%

84% of respondents have not visited a dermatologist.

Do you pay attention to your moles (change in shape, size, texture and color)?

Options	Frequency	Percentage
Yes	27	54%
No	23	46%
Total	50	100%

Table show that 54% pay attention to skin blemishes

Would you use an application that helps you examine moles by taking pictures to prevent the risk of skin cancer?

Options	Frequency	Percentage
Yes	38	76%
No	12	24%
Total	50	100%

Table show that 76% are interested in using a prognosis application of skin cancer.

Point out which of these skin types you think is yours.

Options	Frequency	Percentage
I burn very easily with the sun	23	46%
I sometimes get a sunburn	22	44%
I almost never burn with the sun	5	10%
I never burn with the sun	0	0%

Total	50	100%

Do you avoid the sun between 11 to 14 hours?

Options	Frequency	Percentage
Always	11	22%
Usually	16	32%
Hardly ever	15	30%
Never	8	16%
Total	50	100%

Do you have kids?

Options	Frequency	Percentage
Yes	30	60%
No	20	40%
Total	50	100%

Do you think it is necessary for children to protect themselves from the sun?

Options	Frequency	Percentage
Yes	30	100%
No	0	0%
Total	30	100%

Which of these sunscreen methods does your child use?

Protection	Frequency	Percentage
Sunscreen	24	80%
Hat	30	100%
Long sleeve jersey	23	77%
Sunglasses	2	7%
Umbrella	1	3%
Shadow	21	70%
None	0	0%

Once your child was exposed to the sun, he presented:

Options	Frequency	Percentage
Redness	28	93%
Burning	3	10%
Blisters	0	0%
Peeling	16	53%

Annex 4. Python Code for the software application

A. Preprocessing code

```
import numpy as np
import cv2
def adjust_gamma(image, gamma=1.0):
        invGamma = 1.0 / gamma
        table = np.array([((i / 255.0) ** invGamma) * 255
                for i in np.arange(0, 256)]).astype("uint8")
        return cv2.LUT(image, table)
def processing(file):
    image = cv2.imread(file)
    image = cv2.resize(image, (200,200), interpolation = cv2.INTER_AREA)
    gamma = adjust_gamma(image, gamma=1.5)
    blur2 = cv2.bilateralFilter(gamma,3,25,75)
    cv2.imwrite('save.jpg',blur2)
    cv2.waitKey(0)
    cv2.destroyAllWindows()
```

B. CNN code (trainning, validation and testing)

```
import os
import numpy as np
from tensorflow.python.keras.preprocessing.image import ImageDataGenerator
from tensorflow.python.keras import optimizers
from tensorflow.python.keras.models import Sequential
from tensorflow.python.keras.layers import  Convolution2D, MaxPooling2D
from tensorflow.python.keras import backend as K
from keras.utils.np_utils import to_categorical
K.clear_session()
```

```
data_entrenamiento = './data/entrenamiento'
data_validacion = './data/validacion'
data_test = './data/test'

epocas=500
longitud, altura = 200,200
batch_size=10
pasos =20
validation_steps =10
tamano_filtro = (3,3)
tamano_pool = (2,2)
clases = 4
lr = 0.00001

entrenamiento_datagen = ImageDataGenerator(
    rescale=1. / 255,
    shear_range=0.3,
    zoom_range=0.3,
    horizontal_flip=True)
validacion_datagen = ImageDataGenerator(rescale=1. / 255)
test_datagen = ImageDataGenerator(rescale=1. / 255)

entrenamiento_generador = entrenamiento_datagen.flow_from_directory(
    data_entrenamiento,
    target_size=(longitud, altura),
    batch_size=batch_size,
    class_mode='categorical')

validacion_generador = validacion_datagen.flow_from_directory(
```

```
    data_validacion,
    target_size=(longitud, altura),
    batch_size=batch_size,
    class_mode='categorical')

test_generador = test_datagen.flow_from_directory(
    data_test,
    target_size=(longitud, altura),
    batch_size=batch_size,
    class_mode='categorical')

cnn = Sequential()
cnn.add(Convolution2D(32, tamano_filtro, padding ="same", input_shape=(longitud,
altura, 3), activation='relu'))
cnn.add(MaxPooling2D(pool_size=tamano_pool))
cnn.add(Convolution2D(64, tamano_filtro, padding ="same"))
cnn.add(MaxPooling2D(pool_size=tamano_pool))
cnn.add(Convolution2D(128, tamano_filtro, padding ="same"))
cnn.add(MaxPooling2D(pool_size=tamano_pool))
cnn.add(Convolution2D(128, tamano_filtro, padding ="same"))
cnn.add(MaxPooling2D(pool_size=tamano_pool))
cnn.add(Convolution2D(128, tamano_filtro, padding ="same"))
cnn.add(MaxPooling2D(pool_size=tamano_pool))
cnn.add(Flatten())
cnn.add(Dense(300, activation='relu'))
cnn.add(Dropout(0.5))
cnn.add(Dense(clases, activation='softmax'))

cnn.compile(loss='categorical_crossentropy',
          optimizer=optimizers.Adam(lr=lr),
```

```
        metrics=['accuracy'])
H=cnn.fit_generator(
    entrenamiento_generador,
    steps_per_epoch=pasos,
    epochs=epocas,
    validation_data=validacion_generador,
    validation_steps=validation_steps)

#Save model
target_dir = './modelo1/'
if not os.path.exists(target_dir):
  os.mkdir(target_dir)
cnn.save('./modelo1/modelo1.h5')
cnn.save_weights('./modelo1/pesos1.h5')

#Testing
test_loss,test_acc= cnn.evaluate_generator(test_generador)
print ("Test Accuracy:",test_acc)
print ("Test Loss:",test_loss)
```

C. CNN code (prediction)

```
import numpy as np
from keras.preprocessing.image import load_img, img_to_array
from tensorflow.keras.models import load_model

longitud, altura = 200, 200
modelo = './modelo1/modelo1.h5'
pesos_modelo = './modelo1/pesos1.h5'
cnn = load_model(modelo)
```

```
cnn.load_weights(pesos_modelo)

def predict(file):
  x = load_img(file, target_size=(longitud, altura))
  x = img_to_array(x)
  x = np.expand_dims(x, axis=0)
  array = cnn.predict(x)
  result = array[0]
  answer = np.argmax(result)
  if answer == 0:
    return("Prediagnostic:BASAL CELL CARCINOMA \nThere is a possibility that you have this type \nof skin cancer.Approach a dermatologist to \nconfirm your diagnosis.")
  elif answer == 1:
    return("Prediagnostic:BENIGN \nYour injury looks healthy. \nHowever, do not forget to continue monitoring it \n and if you notice any change in its size, color \nor shape,go to a dermatologist.")
  elif answer == 2:
    return("Prediagnostic:MELANOMA \nThere is a possibility that you have this type \nof skin cancer.Approach a dermatologist to \nconfirm your diagnosis.")
  elif answer == 3:
    return("Prediagnostic:SQUAMOUS CELL CARCINOMA \nThere is a possibility that you have this type \nof skin cancer.Approach a dermatologist to \nconfirm your diagnosis.")
```